

Travail de fin d'études et stage[BR]- Travail de fin d'études : Decarbonizing Western Europe: an optimal Integration of Renewable Fuels and Hydrogen Networks in Transitioning to Net Zero Emissions[BR]- Stage d'insertion professionnelle : ULiège

Auteur : Jacquemin, Julien

Promoteur(s) : Quoilin, Sylvain

Faculté : Faculté des Sciences appliquées

Diplôme : Master en ingénieur civil électromécanicien, à finalité spécialisée en énergétique

Année académique : 2022-2023

URI/URL : <http://hdl.handle.net/2268.2/18053>

Avertissement à l'attention des usagers :

Tous les documents placés en accès ouvert sur le site le site MatheO sont protégés par le droit d'auteur. Conformément aux principes énoncés par la "Budapest Open Access Initiative"(BOAI, 2002), l'utilisateur du site peut lire, télécharger, copier, transmettre, imprimer, chercher ou faire un lien vers le texte intégral de ces documents, les disséquer pour les indexer, s'en servir de données pour un logiciel, ou s'en servir à toute autre fin légale (ou prévue par la réglementation relative au droit d'auteur). Toute utilisation du document à des fins commerciales est strictement interdite.

Par ailleurs, l'utilisateur s'engage à respecter les droits moraux de l'auteur, principalement le droit à l'intégrité de l'oeuvre et le droit de paternité et ce dans toute utilisation que l'utilisateur entreprend. Ainsi, à titre d'exemple, lorsqu'il reproduira un document par extrait ou dans son intégralité, l'utilisateur citera de manière complète les sources telles que mentionnées ci-dessus. Toute utilisation non explicitement autorisée ci-avant (telle que par exemple, la modification du document ou son résumé) nécessite l'autorisation préalable et expresse des auteurs ou de leurs ayants droit.



DECARBONIZING WESTERN EUROPE: AN
OPTIMAL INTEGRATION OF RENEWABLE FUELS
AND HYDROGEN NETWORKS IN TRANSITIONING
TO NET ZERO EMISSIONS.

Author:
JACQUEMIN Julien

Supervisor:
QUOILIN Sylvain

Jury Members:
PAOLO Thiran
DEWALLEF Pierre
LEMORT Vincent
CORNÉLUSSE Bertrand

MASTER'S THESIS COMPLETED IN ORDER TO OBTAIN THE DEGREE OF MASTER OF
SCIENCE IN ELECTROMECHANICAL ENGINEERING MAJOR IN ENERGETICS

University of Liège - School of Engineering and Computer Science
Academic Year 2022-2023

Acknowledgement

For the many hours spent together in the rush of writing, working hard though almost having fun, and always finding the right moments to cheer us up, I want to thank my friends. A special thank you to Guillaume Ploumen and Natalia Kozłowska for all those great moments spent together throughout the year.

I would like to thank Sylvain Quoilin for the always positive and encouraging meetings I have had with him, and Paolo Thiran for the numerous feed-backs he has given me throughout my work.

As this master's thesis marks the apogee of 5 years spent as a student, I would like to thank my parents, without whom none of this would have been even slightly as easy.

I would also like to acknowledge that computational resources have been provided by the Consortium des Équipements de Calcul Intensif (CÉCI), funded by the Fonds de la Recherche Scientifique de Belgique (F.R.S.-FNRS) under Grant No. 2.5020.11, and by the Walloon Region. Additionally, I want to express special thanks to the support team who helped me through some rough times during software installations.

Furthermore, I acknowledge that certain paragraphs have been rephrased for clarity with the assistance of the AI model *ChatGPT*.

Finally, I would like to stress that energy demand data gathered for this work and codes used to provide pre- and post-processing can be found on the github project at https://github.com/Julien-Jacquemin/EnergyScope_multi_cells/tree/preprocessing.

Abstract

Recent developments in the European Union’s energy strategy have highlighted the significance of renewable fuels for the sustainability of the continent’s energy system. However, their diverse production methods and end-use possibilities, along with untapped cross-sectoral synergies, call for energy modeling to identify optimal pathways for renewable fuel production and utilization. With hydrogen emerging as a foundational energy vector for these fuels, and recognizing the critical role of energy interconnections in Europe, a hydrogen network has the potential to be a powerful tool in a decarbonized energy system. To comprehend the complex mechanisms driving the energy transition, we analyze the potential roles of each renewable fuel and hydrogen interconnections as we increase CO₂ emission restrictions. This study encompasses the electricity, buildings, transport, agriculture, and industry sectors across Western Europe, employing an hourly time resolution to fully capture the potential of those fuels within a system with high shares of renewables. The analysis employs the EnergyScope MultiCell model, which enables integrated optimization of the energy system, spanning from resource utilization to the selection of end-use technologies. The findings reveal that while renewable fuels entail a substantial increase in system costs, they prove effective in reducing the final 20% of emissions, using 1990 emission levels as a reference. Furthermore, they empower Western Europe to achieve self-sufficiency, even without negative CO₂ technologies. As hydrogen production reaches 3300 TWh, a hydrogen network facilitates the energy transition by reducing its costs by 14.5% (60 b€/year). Despite this, gas infrastructures remain valuable assets, with only 45% of hydrogen interconnections being retrofitted gas pipelines, underscoring their importance for renewable gas exchanges.

Contents

1	Introduction	1
1.1	Context	1
1.2	Energy System Models	2
1.3	EnergyScope MC and Scope of this Work	4
2	Model Description	5
2.1	Origins and Evolution	5
2.2	Inputs	6
2.2.1	Demands	6
2.2.2	Resources	7
2.2.3	Technologies	7
2.3	Working Principle	8
2.4	Regions and Macrocells	10
2.5	Program Structure	11
3	Methodology	12
3.1	International shipping	13
3.1.1	Demand	13
3.1.2	Technologies	13
3.2	Aviation	15
3.2.1	Demand	15
3.2.2	Technologies	15
3.3	Steel	16
3.4	Conversion technologies	17
3.4.1	Bio-fuels	17
3.4.2	Electro-fuels	19
3.5	Hydrogen network	20
3.5.1	Model Philosophy	21
3.5.2	Practical implementation in EnergyScope MC	23
4	Data collection	28
4.1	International shipping	28
4.1.1	Demand	28

4.1.2	Technologies	30
4.1.3	Sources and methodologies	31
4.2	Aviation	31
4.2.1	Demand	31
4.2.2	Technologies	33
4.2.3	Sources and methodology	33
4.3	Steel	34
4.3.1	Demand	34
4.3.2	Technologies	35
4.3.3	Sources and methodologies	36
4.4	Conversion technologies	36
4.5	Networks	38
4.5.1	Exchange networks	38
4.5.2	Domestic network	40
4.5.3	Sources and methodology	40
5	Simulations	43
5.1	Scenarios	43
5.2	Sensitivity Analysis	44
5.2.1	Discount rate	44
5.2.2	Methanol exchange capacities	45
6	Results and discussion	46
6.1	System Design	46
6.2	System Cost	47
6.2.1	Impact of CO ₂ Emissions Reduction	47
6.2.2	Impact of Hydrogen Network	51
6.3	Utilization of renewable fuels	54
6.3.1	Ammonia	55
6.3.2	Methanol	56
6.3.3	Synthetic Fuel	56
6.3.4	Hydrogen	57
6.4	Storage Technologies	59
6.5	Energy Exchanges	60
6.5.1	Reference Scenario	60
6.5.2	Impact of decreasing methanol exchange capacity.	63
6.6	Impact of the Discount Rate on Decarbonization	64
7	Conclusion	67

A	How to extend EnergyScope MC	69
A.1	How to introduce a new EUD	69
A.2	How to introduce a new EUT	69
A.3	How to introduce a new technology	70
B	Minor modifications to EnergyScope MC	71
C	Additional tables and figures	72
C.1	Tables	72
C.2	Figures	76

List of Figures

1.1	FEC versus EUD based energy models.	3
2.1	Structure of demand in EnergyScope MC.	7
2.2	Conceptual example of a simplified energy system in EnergyScope TD, based on G. Limpens [12].	8
2.3	Conceptual example of a simplified energy system in EnergyScope MC, based on G. Limpens [12] and adapted by P.Thiran in [16].	9
2.4	Process of picking and using typical days in EnergyScope MC, for a sim- plified setup. Made by P. Thiran [16].	10
2.5	Aggregated regions considered in the model.	11
3.1	Summary of the implementation of synthetic fuels layers and related con- version technologies.	18
3.2	Interconnection patterns for the three exchange networks considered in the model.	23
4.1	Projected EU international maritime freight demand per country for the year 2035, in Gtkm/year.	29
4.2	Projected EU aviation demand for 2035, in Gpkm/year.	32
4.3	European steel production per country in 2021, in Mt/year.	35
6.1	Sankey diagram for the yearly operation of the global optimized system, with 0 CO ₂ emissions.	47
6.2	Evolution of system total price with increasing percentage of CO ₂ emissions reduction, compared to 1990.	48
6.3	Allocation of system cost difference between 0% and 100% CO ₂ emissions, categorized by groups.	49
6.4	Cost of a ton of CO ₂ as a function of emissions reduction compared to 1990 levels.	50
6.5	Evolution of the system cost with increasing value for the maximum bound on the transfer capacity for hydrogen.	52
6.6	Allocation of system cost difference between the with and without hydrogen exchanges scenario, for a net zero scenario, categorized by group.	53

6.7	Comparison between scenarios with and without hydrogen interconnections, for a 100% emission reduction.	54
6.8	Ammonia production methods and consumption sectors.	55
6.9	Methanol production methods and consumption sectors.	56
6.10	Synthetic fuels production methods and consumption sectors.	57
6.11	Hydrogen production methods and consumption sectors.	59
6.12	System daily and seasonal storage capacities as a function of the decarbonization ratio.	60
6.13	Yearly exchange of energy carrier (Hydrogen, gas and electricity) between regions in the reference scenario.	62
6.14	Yearly exchange of methanol for the reference scenario and when constraining additional freight capacity related to energy exchange to 6 GW.	64
6.15	Yearly exchange of gas for the reference scenario and when constraining additional freight capacity related to energy exchange to 6 GW.	64
6.16	Influence of the discount rate on the system cost (normalized) and the share of CAPEX and OPEX in the total system cost, with increasing decarbonization ratio.	66
C.1	Sankey diagram for the yearly operation of the global optimized system, with CO ₂ emission levels of 1990.	76
C.2	Cumulated load profile of hydrogen interconnections for a value of $t_{c_{mul}}$ equals to 2.	76

List of Tables

4.1	Parameters common to all cargo shipping technologies implemented in the model (Tonnage is different for retrofitted ammonia and methanol ships). .	30
4.2	Costs, shipping capacities, and fuel consumptions of the implemented shipping technologies.	30
4.3	Sources and methodologies for international maritime freight demand and technologies.	31
4.4	Main model parameters and intermediate parameters for the implemented aviation technologies.	33
4.5	Sources and methodologies for aviation demand and technologies.	34
4.6	Inputs and outputs of the different production routes considered for steel making.	35
4.7	Main model parameters for the different routes considered for steel production.	36
4.8	Sources and methodologies for steel supply and production technologies. . .	36
4.9	Main parameters for the conversion technologies implemented in the model.	36
4.10	Input and output for the conversion technologies implemented in the model. ¹	37
4.11	Sources and methodologies for conversion technologies characteristics. . . .	38
4.12	Costs and geographic characteristics of the hydrogen pipelines considered in the model, for new and repurposed pipelines.	39
4.13	Economic parameters for the gas and electricity exchange networks.	39
4.14	Maximum capacities of reference for hydrogen interconnections between countries, in GW ⁹	40
4.15	Economic parameters for the domestic hydrogen network. ¹⁰	40
4.16	Sources and methodologies for network characteristics.	42
6.1	Gas and hydrogen exchange network design.	63
C.1	Summary of pipeline costs, capacities and Capacity-& distance weighted share of the hydrogen backbone, for different pipeline typologies.	72
C.2	Summary of pipeline costs, capacities and Capacity-& distance weighted share of the hydrogen backbone, for different pipeline typologies.	72
C.3	Rate of aviation demand increase.	73

C.4	Change in the installed capacity of various technologies and in energy import quantities when changing the discount rate from 5 to 10%, for various emissions reduction targets.	75
-----	--	----

List of Abbreviations

EUD End-Use Demand

FEC Final Energy Consumption

EUT End-Use Type

EnergyScope MC EnergyScope Multi-Cell

EnergyScope TD EnergyScope Typical Days

HVC High-Value Chemical

NED Non-Energy Demand

EHB European Hydrogen Backbone

GHG Green House Gas

TEU Twenty Equivalent Unit

NG Natural Gas

LFO Light Fuel Oil

LNG Liquified Natural Gas

LH2 Liquified Hydrogen

HEFA-SPK Hydro-processed Esters and Fatty Acids Synthetic Paraffinic Kerosene

AtJ Alcool to Jet

FT Fischer-Tropsch

FC Fuel Cell

EAF Electric Arc Furnace

DRI Direct Reduced Iron

BF-BOF Blast Furnace-Basic Oxygen Furnace

PtL Power to Liquid

OPEX Operating Expenditure

CAPEX Capital Expenditure

Chapter 1

Introduction

1.1 Context

Aligned with the Paris Agreement’s commitment to limit global temperature rise to well below 2°C [1], the European Union (EU) has set its climate strategy in motion with the European Green Deal, aiming for a net-zero CO₂ emissions EU by 2050 [2]. To solidify its dedication to these goals, the EU enshrined them into law through the European Climate Law, along with a newly established target: a 55% reduction in CO₂ emissions by 2030 [3]. In response to this milestone, the EU’s strategy has evolved with the introduction of the Fit for 55 package.

The Fit for 55 package comprises a series of proposals aimed at revising and updating the EU legislation [4]. Notably, three documents—Alternative Fuels Infrastructure (AFIR), ReFuelEU Aviation, and FuelEU Maritime—highlight the crucial role of alternative fuels in the transport sector, which accounts for over a quarter of the EU’s emissions.

Subsequent to Russia’s military aggression in Ukraine, the EU unveiled the RePowerEU plan, seeking to reduce its reliance on fossil fuels from Russia [5]. This plan underscores the urgent need to transition from fossil fuels to renewable alternatives and highlights the necessity for developing hydrogen infrastructure, particularly a pan-European hydrogen network.

Given the anticipated prominence of renewable fuels in the future European energy system, energy modeling becomes essential to ascertain optimal utilization strategies for each fuel. The diversity of renewable fuel production pathways, coupled with distinct suitability for specific end-uses and the complex interactions between energy sectors, necessitates energy system modeling to guide decision-making and determine the most promising pathways.

Within the interconnected European energy system, cross-border energy exchanges

play a pivotal role. These exchanges offer enhanced integration of renewable energy sources by connecting regions with diverse weather conditions, mitigating energy availability intermittency. Furthermore, they facilitate energy production in economically viable locations and its transportation to consumption centers. Importantly, such exchanges contribute to the EU’s net-zero emission objectives by enabling countries with insufficient renewable potential to access renewable resources from other nations [6]. Given the possible significance of hydrogen in low-emission energy systems, it is imperative to model energy exchanges, particularly analyzing the impact of hydrogen exchanges on the EU energy landscape.

In conclusion, the adoption of renewable fuels is set to accelerate in the forthcoming years. To construct a sustainable, efficient, and independent EU energy system, it is imperative to identify optimal production pathways for renewable fuels and delineate their most suitable applications. Additionally, considering the projected roles of energy exchanges and hydrogen, a comprehensive analysis of their impacts on the energy system and the optimal design of a European hydrogen network is warranted.

1.2 Energy System Models

A wide range of open-source models suitable for conducting such analyses are available. Examples of such models include *Pypsa Eur*¹ [7], *GENeSYS-MOD*² [8], and *JRC-EU-TIMES*³ [9]. However, each model possesses unique characteristics that render it more or less suitable for specific tasks.

Although *Pypsa Eur* and *GENeSYS-MOD* can comprehensively model cross-sectoral interactions, they adopt a representation based on Final Energy Consumption (FEC) for the energy demand. In this approach, the quantity of each fuel required to fulfill the demand in a given sector is predetermined prior to optimization. This presupposition stems from the assumption that certain end-use technologies will dominate specific domains, while others will not. However, predicting the leading technologies in a future energy system hinges not only on technological attributes but also on regional resource availability, fuel supply chain costs, demand scale, and potential alternative uses of the fuel across sectors. Consequently, making assumptions about fuel types and quantities for end-use leads to considerable uncertainties when seeking to determine the optimal system configuration.

A solution to this challenge lies in representing demand using an end-use demand (EUD) framework, as adopted by the *JRC-EU-TIMES* model. EUD signifies the energy

¹<https://github.com/PyPSA/pypsa-eur>

²<https://git.tu-berlin.de/genesysmod/genesys-mod-public/-/releases/genesysmod3.0>

³<https://data.jrc.ec.europa.eu/collection/id-00287>

or service that directly reaches the consumer. For instance, while the energy consumed by a heat pump to warm a house constitutes the FEC, the actual heat delivered into the building constitutes the EUD. Adopting the EUD perspective enables the consideration of diverse technologies to fulfill this heat demand, including options such as a gas burner, heat pump, or electric heater. Figure 1.1 illustrates the distinction between the FEC and EUD energy system approaches.

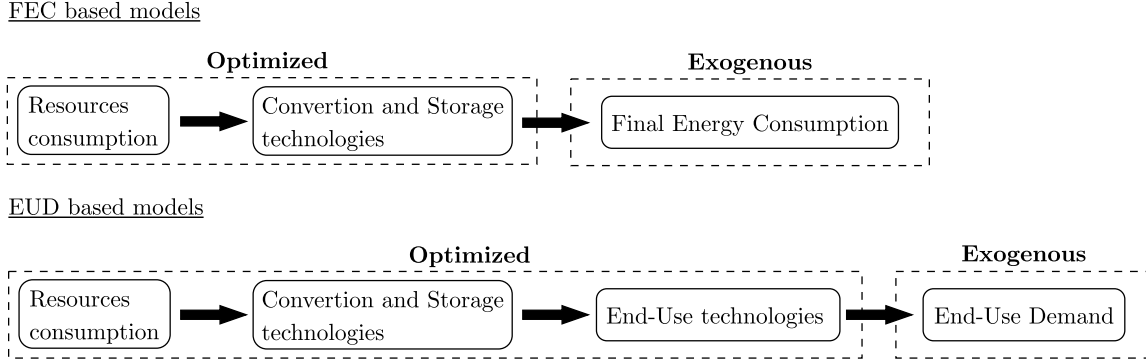


Figure 1.1: FEC versus EUD based energy models.

However, both the *JRC-EU-TIMES* and *GENeSYS-MOD* models represent variations in resource availability and energy consumption using time-slices, rather than dividing the year into discrete hourly blocks. For instance, in the *JRC-EU-TIMES* model, a year is segmented into 12 time-slices, with three slices allocated to each season. Within each season, one slice corresponds to daytime, another to nighttime, and the final slice to the peak consumption period. However, this approach is less effective in capturing the intermittency inherent in renewable energy sources like wind and solar power. Consequently, these models are less well-suited for analyzing the integration of renewable technologies compared to methods with higher temporal resolution.

On the other hand, *EnergyScope MC*⁴ adopts an EUD framework for representing energy demand, enabling the optimization of the mix of end-use technologies. Additionally, this model divides the year into hourly intervals with the help of typical days. This approach allows for the incorporation of short-term fluctuations in energy production and consumption, enhancing the analysis of challenges related to the integration of renewable energy. The distinctive characteristics of *EnergyScope* render it highly suitable for exploring the potential of renewable fuels within the optimally designed future energy system.

For a more comprehensive comparison of energy models, please refer to M.G. Prina et al. [10].

⁴https://github.com/energyscope/EnergyScope_multi_cells

1.3 EnergyScope MC and Scope of this Work

With its end-use demand (EUD) representation of energy demand and its high temporal resolution, EnergyScope MC emerges as an optimal model for conducting the envisioned analysis. However, it currently lacks certain essential features required for a comprehensive characterization of the renewable fuel sector. Indeed, as highlighted in this report, renewable fuels are foreseen to play a major role in the decarbonization of international maritime shipping and aviation. Moreover, hydrogen is recognized to have a crucial role for mitigating CO₂ emissions in the challenging task of decarbonizing steel production. However, these three sectors are not yet implemented in the current version of the model. Additionally, as most renewable fuels can be produced efficiently from hydrogen, the consideration of hydrogen exchange between nations becomes pertinent. Considering a hydrogen network within the optimization is therefore necessary. Lastly, it's important to note that the model currently incorporates only a limited number of conversion technologies capable of producing synthetic fuels. Conversion technologies should be represented in an exhaustive manner to ensure that every existing production pathway is considered when designing the optimal system.

In preparation for conducting an analysis of the future European energy system, it is imperative to extend the model's capabilities by integrating the features mentioned above. This expansion is necessary to ensure that the results derived from the analysis are both robust and meaningful.

Chapter 2

Model Description

2.1 Origins and Evolution

EnergyScope MultiCell (EnergyScope MC) finds its origins in the work of S. Moret on how uncertainty impacts strategic energy planning [11]. The model has then a monthly time resolution and is used for the strategic energy planning of urban and regional energy systems. G. Limpens et al. carried this work forward, extending it into EnergyScope Typical Days (EnergyScope TD), which encompassed a broader array of technologies and demands. The transition to an hourly time resolution further facilitated the study of intermittent renewable energy integration and storage dynamics. Following its utilization in Switzerland [12], the model was adapted to Belgium, unraveling potential energy transition pathways [13]. Later, J. Dommissse and J.L. Tychon employed EnergyScope TD to model energy dynamics in 26 European countries [6], revealing that specific nations, including Slovenia, Italy, Germany, the Netherlands, and Belgium, might be unable to meet their energy demands solely through their domestic renewable potential. On the other hand, other countries possess renewable surpluses relative to their consumption. Addressing this disparity, A. Hernandez and P. Thiran extended the model to EnergyScope MC, which introduced the concept of energy carrier exchanges in multi-regional systems. The initial application of EnergyScope MC considered France, Belgium, and Switzerland [14]. To manage computational complexity in larger-scale models, an innovative approach was adopted, merging similar countries into macro-cells for modeling Western Europe [15]. EnergyScope MC continues to evolve, with P. Thiran leading its ongoing development.

EnergyScope MultiCell is an open source, multi-sectoral, and multi-region energy model used to optimize the investment and operation cost of an entire energy system, such as the European one. It is a powerful tool to analyze the complex interactions between different energy sectors in different interconnected regions. This section aims at describing the working principles of the model in order to understand better how it was extended to fit the objectives of this work.

2.2 Inputs

2.2.1 Demands

The model covers the demands for electricity, high-temperature heat, low-temperature heat, space cooling, process cooling, passenger mobility, freight mobility, and non-energy materials, across the households, services, industrial, and transportation sectors. These demands are represented in the model as End Use Demands (EUD), which differs from the Final Energy Consumptions (FEC). The FEC is *"the energy that reaches the final's consumer's door"*, as defined by the European Commission, while the EUD is the demand that is met using the FEC. As an example, in the context of mobility, the EUD might be the number of kilometers traveled by a person, while the FEC would be the energy consumed by the car he is using. This way of representing the demand allows for considering a broad range of possible technologies, with different inputs, efficiencies, prices, etc, to satisfy the EUD. In the example, the car could run on diesel, gasoline, hydrogen, electricity, etc. The technologies leading to a system-wide optimal solution can therefore be chosen.

Each region modeled has its own specific demand and data for 26 European countries have been gathered by J. Dommissé and J.L. Tychon, with the methodology explained in [6]. For each region, each demand is represented by a consumption value per year, as well as an hourly time series giving the ratio of the yearly demand that has to be met at a specific hour, for demands that are time-dependent. Demands that are not time-dependent are the freight mobility and the non-energy demands and they are equally distributed through the hours of the year.

Each EUD is finally further categorized into End Use Types (EUTs). The proportion of an EUD covered by each of its EUTs is an optimized variable taking values in previously defined intervals. Every EUT is then attributed an exclusive set of technologies able to satisfy it, called *"the technologies of end-use type"*. Each technology can also be given a minimum and maximum value for the proportion of their EUT that they have to satisfy. The concepts of sectors, EUDs, and EUTs are represented in figure 2.1.

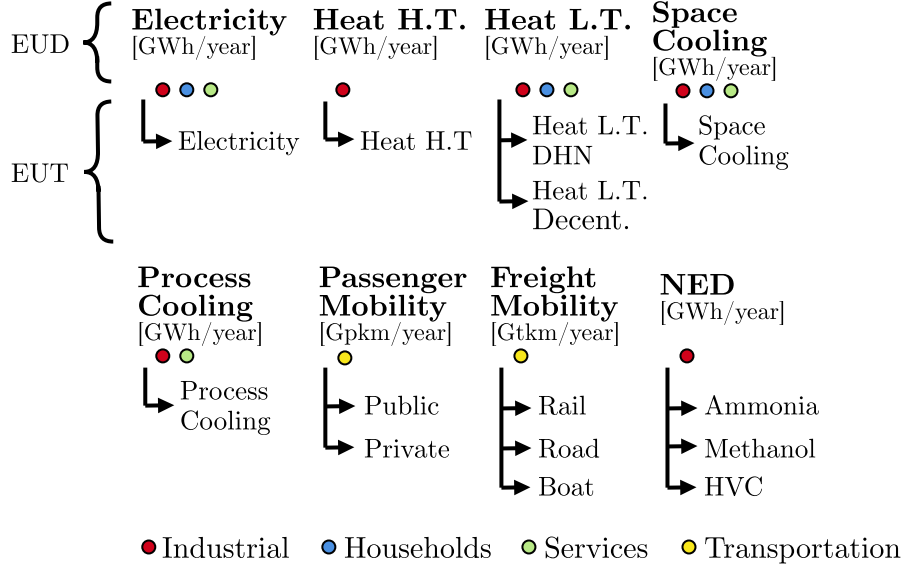


Figure 2.1: Structure of demand in EnergyScope MC. Abbreviations: "EUD": End-use demand, "EUT": End-use type, "Heat H.T.": High-temperature heat, "Heat L.T. DHN": Low-temperature district heat network, "Heat L.T. Decent.": Decentralized low-temperature heat, "HVC": High-value chemicals, "NED": Non-energy demand.

2.2.2 Resources

Resources constitute the inputs supplied to the system to fulfill demands. These resources may originate locally within regions and/or be imported from external sources. In both cases, they are subject to defined maximum availability. Each resource is characterized by local and external prices, as well as a CO₂ content. The total CO₂ emissions of the system are computed by aggregating the CO₂ content of all utilized resources.

2.2.3 Technologies

Technologies are categorized into distinct groups. First, there are end-use type technologies with outputs directly used to satisfy the EUTs. Storage technologies retain energy in specific forms for subsequent release in the same form. Infrastructure technologies encompass diverse technologies, including network-related and conversion technologies that transform one energy vector into another. Bounds can be set on EUTs to constrain the coverage of their EUD within specific ranges. Additionally, maximum and minimum installed capacities can be specified for each technology.

Renewable technologies relying on intermittent energy sources are accompanied by time series indicating hourly load factors throughout the year. The maximum installed capacity for these technologies is calculated based on available land space in the country and is a fixed parameter within the model.

2.3 Working Principle

The working principle of the program is centered around the concept of layers. A layer represents a quantity that has to be balanced at every time step. The set of layers is the union between all the possible energy vectors considered in the model and the EUTs. Each type of energy vector, such as wood, ammonia, gas, solar irradiation, etc., must satisfy an energy balance between its inflow and outflow. Similarly, each EUT functions as a layer, as it must fulfill demands at each time step using the technologies assigned to fulfil it.

The concepts explained above are illustrated in figure 2.2.

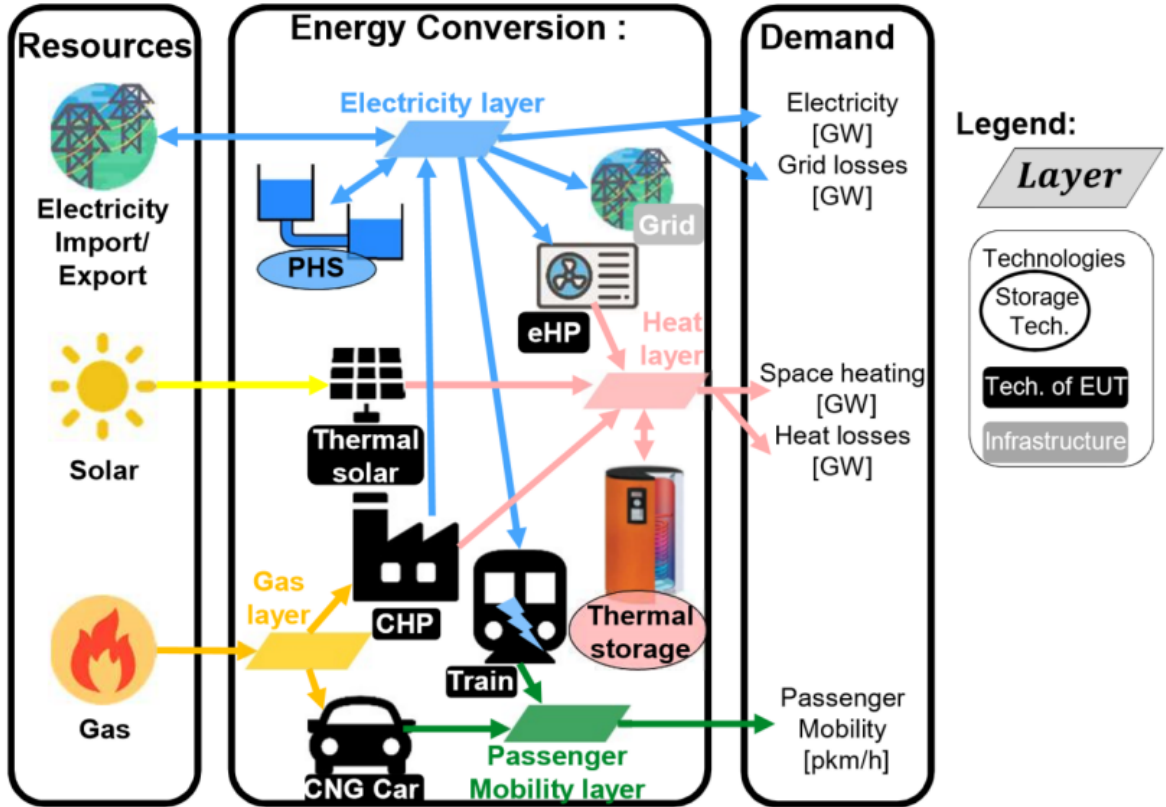


Figure 2.2: Conceptual example of a simplified energy system in EnergyScope TD, based on G. Limpens [12]. Abbreviations: pumped hydro storage (PHS), electrical heat pump (eHP or HP), combined heat and power (CHP), compressed natural gas (CNG). Some icons are made by Freepik from www.flaticon.com

The program employs linear optimization to determine the set of resources and technologies that minimizes the system cost while satisfying constraints. The resulting installed capacities and optimal operation can be extracted. Optimization constraints are resolved hourly for each individual region, enabling the consideration of renewable energy source intermittence. In the multi-cell version, regions can exchange resources, as demonstrated in Fig. 2.3.

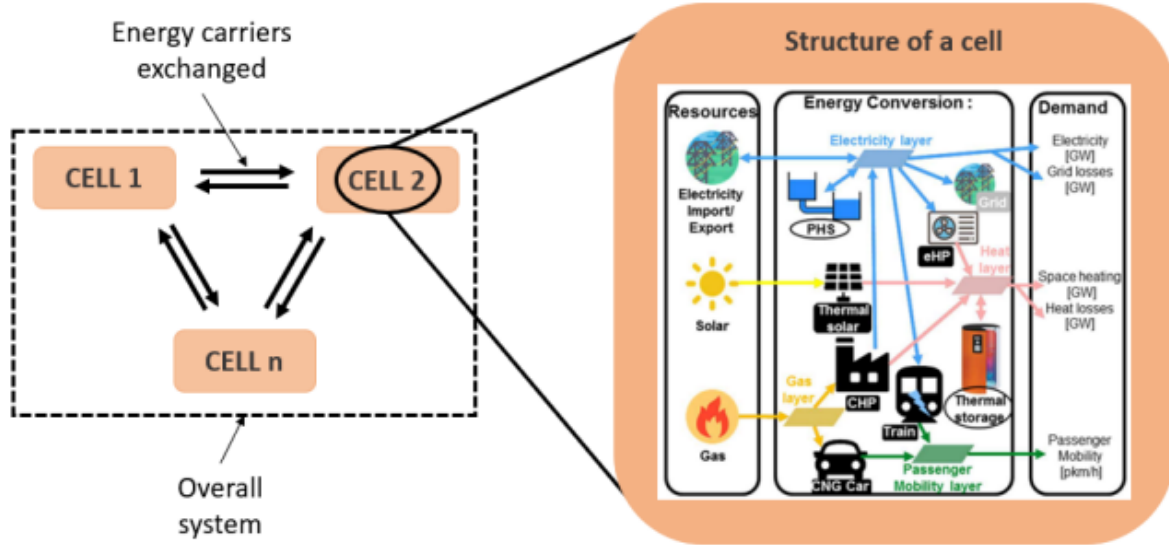


Figure 2.3: Conceptual example of a simplified energy system in EnergyScope MC, based on G. Limpens [12] and adapted by P. Thiran in [16]. Abbreviations: pumped hydro storage (PHS), electrical heat pump (eHP or HP), combined heat and power (CHP), compressed natural gas (CNG). Some icons are made by Freepik from www.flaticon.com

Due to a computational time constraint, the optimization is performed not for each hour of the year, but for a specific number of representative days referred to as *typical days*. The optimal number of typical days results from a trade-off between accurate energy system representation and computational time. The selection of these days is achieved through a MILP formulation of the k-medoid method, as elaborated in [12] and adapted for EnergyScope MC in [14]. This method utilizes time series of EUTs and of technologies based on intermittent sources to identify days that best represent the majority of the year. EnergyScope TD demonstrated that 12 typical days strike a balance between accuracy and computational time. However, in the multi-cell version, dealing with multiple regions implies dealing with multiple sets of time series which are not 100% correlated throughout the days of the year. This fact makes fewer and fewer days look like each other and therefore forcefully decreases the accuracy of the representation when compared to using the same number of days with EnergyScope TD. In this work, a number of 14 TD is therefore considered as the best trade-off. A primitive use of typical days would only allow to consider storage on a daily basis. However, as storage plays a major role in energy systems, notably through seasonal storage, storage levels are optimized through all the hours of the year, following a methodology explained in [12]. The overall process of typical days selection and optimization is picture in figure 2.4

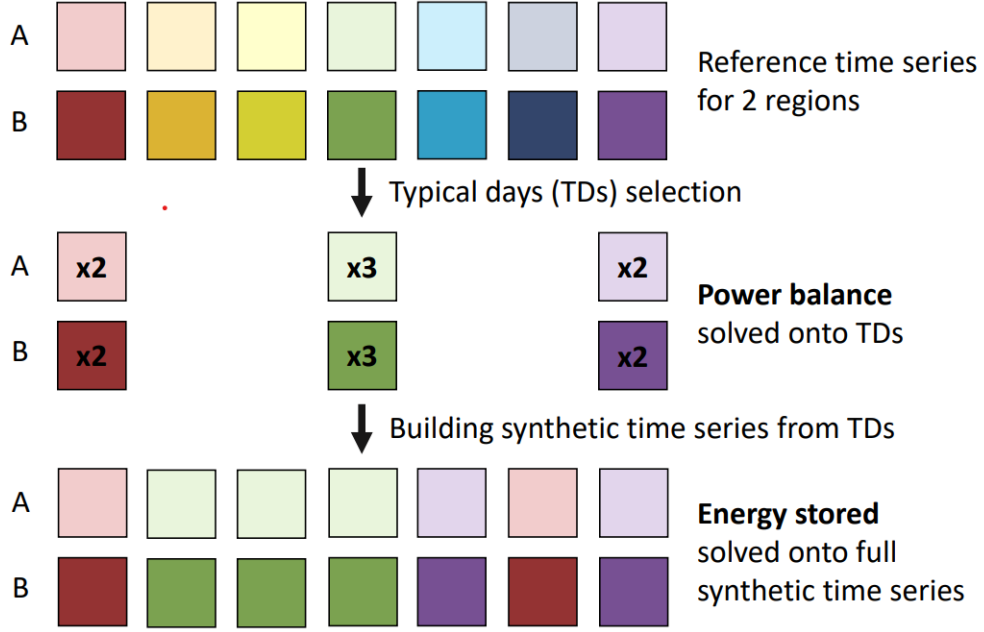


Figure 2.4: Process of picking and using typical days in EnergyScope MC, for a simplified setup. Made by P. Thiran [16].

2.4 Regions and Macrocells

This work focuses on modeling several countries, including Austria (AU), Belgium (BE), Denmark (DK), France (FR), Germany (DE), Ireland (IE), Italy (IT), the Netherlands (NL), Portugal (PT), Spain (ES), Sweden (SE), Switzerland (CH), and the United Kingdom (UK). To manage computational complexity associated with an increasing number of countries, [15] proposed a methodology for grouping neighboring countries with shared energy-related characteristics. Analyzing renewable potential and demands, they identified the following groups: AT-CH-IT, DK-SE, IE-UK, BE-DE-LU-NL, FR, ES-PT, as depicted in figure 2.5. These countries were merged by aggregating demands and combining hourly time series with specific weights, as elaborated in their publication.

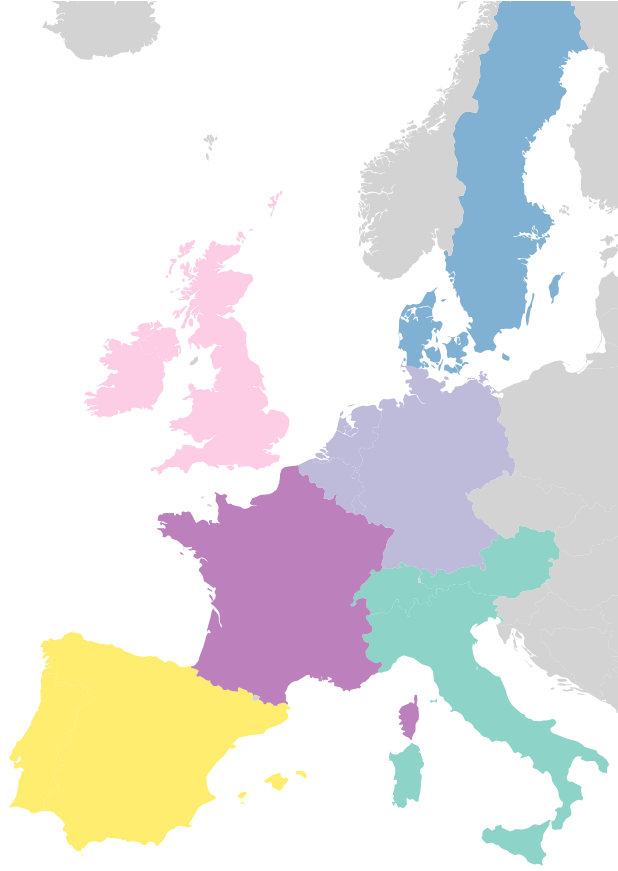


Figure 2.5: Aggregated regions considered in the model.

2.5 Program Structure

The core of the program is built around a linear programming optimization code developed using *AMPL*. This code aims to minimize the annualized cost of the energy system. The optimization problem is solved utilizing the *CPLEX* solver with the barrier algorithm. Input data, organized in *.dat* files, feed into this code. A Python interface facilitates the transformation of *.csv* files into *.dat* files, allowing for specific changes in the inputs and post-processing of results. Each modeled region has a dedicated folder housing its corresponding *.csv* files. Additionally, folders with *.csv* files exist for non-region-specific data and data related to energy carrier exchanges.

Chapter 3

Methodology

It is possible to modify EnergyScopeMC in multiple ways in order to fit the study's intended purpose. One possibility is to change the model parameters to create different scenarios, e.g. changing the maximum CO₂ emission of the regions or modifying the demand of a certain sector. Another possibility is to extend the model to make it more representative of the energy system. This can be done by adding new available technologies, demand, or resources.

To analyze the role of renewable fuels in a future energy system, one should try and implement as many relevant technologies and demands as possible in the model to represent reality in the best way possible. While a broad range of renewable fuels such as renewable diesel, gasoline, gas, ammonia, methanol, etc. are already considered, the model lacks some key elements to represent accurately the production of these fuels and their consumption. According to the international energy agency (IEA), *"Low-emission fuels will be needed to decarbonize parts of the energy system where direct electrification is more difficult or more expensive, such as elements of heavy industry and long-distance transport"* [17]. Also, the European Hydrogen Backbone (EHB) sees a future increase in the demand for hydrogen and hydrogen-derived fuels in the industry for steel making and in heavy road transport and aviation. Finally, maritime companies and shipowners forecast that the future of maritime fuels will be a mix of ammonia and methanol [18].

To account for these forecasts, several features are added to EnergyScopeMC. Demand for international shipping is introduced and related technologies are added. The structure of passenger mobility demand is modified to take into account the demand for intra-EU aviation. Extra-EU aviation demand is added to the system. Several conversion technologies for renewable fuel production are introduced. Finally, a hydrogen network is introduced to take the price of hydrogen transport into account and to model hydrogen exchanges between countries.

3.1 International shipping

International shipping is responsible for 6.7% of oil consumption in the world [19] and accounts for 3.6 % of the world GHG emissions [20]. The international maritime organization (IMO) recently came up with an emission reduction strategy aimed at cutting 40% of the CO₂ emission by 2030 and 70% by 2050, compared to 2008 levels. According to the organization *"It is clear that the global introduction of alternative fuels and/or energy sources for international shipping will be integral to achieve the overall ambitions set out in IMO's initial strategy for reducing GHG emissions from international shipping"* [21]. Given the significance of the energy consumption of international shipping and the key role of renewable fuels in the decarbonization of the sector, it was decided to implement it in the model.

3.1.1 Demand

Freight demand is already part of the model for terrestrial and inland navigation transportation. However, it has been decided to create a new demand for international freight, apart from the already existing one, i.e the international shipping demand is not implemented as an EUT of the freight demand but as a new EUD. Indeed, the modes of transportation used to meet the current freight demand can not be substituted by the inter-continental technologies used to meet the international demand, nor the reverse. Furthermore, merging intra-EU maritime shipping demand with current freight demand and creating new demand for extra-EU shipping can't be done either. This would be motivated by the fact that intra-EU demand and the current demand occur between the same countries in Europe, and one could want to analyze the transfer of technologies from road to maritime shipping, as the latest is more efficient. However, shipping can only happen between coastal countries while the current freight demand makes no distinction between the commercial partner, i.g. Belgium has commercial partners all over Europe, but it can perform shipping only with coastal countries. Maritime shipping technologies and the technologies used to satisfy the current freight demand are therefore not equivalent and it would be delicate to try and analyze the transfer of technologies from one demand to the other.

The steps for introducing a new demand in EnergyScope MC are detailed in Appendix A.1

3.1.2 Technologies

Once the demand has been introduced, end-use technologies have to be added to provide a way of meeting this demand. The type of cargo ship considered for the data collection

is the container cargo ship of 4000 twenty equivalent units (TEU).

First, container cargo is chosen because containers are the second type of cargo most handled in European ports in terms of weight, accounting for 25% of the total gross weight, after liquid bulk with 35.2% [22]. However, liquid bulk cargo ships are not selected as the reference as they are primarily associated with energy import. In the scenarios considered, the potential of Europe to be energetically autonomous is analyzed, and imports of energy should theoretically fall to zero, which would decrease the demand for liquid bulk. The subtraction of the demand linked to energy imports has not been carried out in this work and is a consideration for improvement.

Next, a size of 4000 TEU is chosen because the mean size of container ships is 3420, according to [23]. The closest standard size for container ships is then 4000 TEU.

Regarding fuels, various possibilities are considered. While the majority of ships currently run on heavy or light fuel oil, trends indicate an increase in orders for alternative-fuel capable vessels, including LNG, methanol, as well as ammonia and hydrogen-ready ships [24]. Meanwhile, ammonia and methanol are seen as the future candidates for a zero-emission maritime fleet [25][26], with methanol seen as a more mature technology [27]. Hydrogen would be preferred for international short-sea shipping [28] due to limitations on the range of the vessels. Batteries are ruled out due to their low energy density, allowing only for a very limited range [28].

In terms of engine type, ships can use propulsion provided by an internal combustion engine or via an electric motor powered by a fuel cell. While fuel cells are less mature and more expensive technologies, they offer better fuel efficiency [28]. Finally, there is the possibility of technology conversion, allowing oil-powered ships to be retrofitted into ammonia or methanol ships, at the cost of money and container space [26].

Based on this information, the following technologies have been added to the model:

- CARGO_LFO: container cargo ship running on fuel oil.
- CARGO_LNG: container cargo ship running on LNG.
- CARGO_METHANOL: container cargo ship running on methanol powering an ICE.
- CARGO_AMMONIA: container cargo ship running on ammonia powering an ICE.
- CARGO_FUELCELL_LH2: container cargo ship running on liquefied hydrogen powering a fuel cell.

- CARGO_FUELCELL_AMMONIA: container cargo ship running on ammonia powering a fuel cell.
- CARGO_RETRO_METHANOL: container cargo ship running on methanol, retrofitted from a ship running on fuel oil.
- CARGO_RETRO_AMMONIA: container cargo ship running on methanol, retrofitted from a ship running on fuel oil.

3.2 Aviation

The aviation sector is responsible for over 3.4% of the GHG emissions [20] and consumes 8.6% of the world’s total oil supply [19], a demand for fuel that could be met by renewable aviation fuels and hydrogen.

3.2.1 Demand

Unlike the case of international shipping, aviation demand is divided into extra-EU and intra-EU demand. While extra-EU aviation demand is introduced in the model following the methodology explained in section A.1, intra-EU demand is added as a new EUT, following the methodology explained in section A.2. This approach is motivated by the fact that intra-EU aviation serves a passenger demand that could be met by other means of transportation, such as trains and buses. One could therefore want to model a scenario analyzing a shift from aviation to less intensive means of transportation. In contrast, extra-EU aviation demand cannot be met by any other means of transportation, justifying a separate category of demand.

3.2.2 Technologies

Sustainable aviation fuel could potentially lead to the most significant reduction in the sector’s CO₂ emissions in the short to medium term, as indicated in a report on aviation commissioned by the European Parliament’s Committee on Transport and Tourism [29]. The same source highlights liquified hydrogen as the fuel with the highest projected consumption in aviation by 2050, surpassing renewable kerosene and electricity, offering the potential for complete sector decarbonization. However, it also acknowledges that due to its low energy density, hydrogen will likely be limited to smaller aircraft, at least in the initial stages, making it a long-term option. A similar perspective is shared by [30]. On the other hand, the Eurocontrol Aviation Outlook 2050 [31] anticipates only a 2% share of electric and hydrogen-powered aircraft in its net zero scenario.

There is therefore no clear consensus on the use of hydrogen as a fuel for aviation in the near future. Nonetheless, this work chose to consider hydrogen as a potential fuel for

aviation with various possible technologies put forward in [29]. However, these technologies are in the early stages of development, and further analysis is required to identify the most promising options and obtain reliable performance parameters. Additionally, many of these technologies are projected to become available only by 2035, with the exception of hydrogen-fueled gas turbines, which are forecasted to be available by 2030. Consequently, the model currently incorporates only the hydrogen-fueled gas turbine technology, limited to meeting a maximum of 10% of the intra-EU aviation demand.

The technologies used to meet the demand all pertain to aircraft. However, the model distinguishes between two categories of aircraft: narrow-body jets for intra-EU demand and wide-body jets for extra-EU demand. This differentiation is necessary due to the distinct characteristics of these aircraft types in terms of pricing and fuel consumption.

3.3 Steel

Steel is a strategic sector for the EU economy but it is responsible for 5% of the EU total CO₂ emissions. The industry has performed great achievement in terms of efficiency and is operating close to the optimum levels, meaning that major changes will be necessary to further reduce the sector's emissions. To comply with the EU's target of decarbonizing its economy for 2030 and 2050, the industry appears to be focusing on hydrogen-based steelmaking.

Currently, two main ways to produce steel coexist. The first one involves transforming iron ore through a series of highly energy-intensive processes centered around the blast furnace. The main input for these processes is coal and they would require of it 21 GJ per ton of crude steel. This route accounted for 56% of the global steel production in 2020. In the secondary route, steel scrap is gathered and melted in an electric arc furnace (EAF). The primary energy used for this second route is electricity, but natural gas can provide additional energy input, while some 12kg/t of coal is to be used to increase efficiency and for carburization of the steel.

A last route, whose use is yet negligible in the EU but could lead to a major decarbonization of the system is called "direct reduced iron (DRI-EAF)". This process involves reducing iron ore with hydrogen and carbon oxide obtained from natural gas or coal. The reduced iron is then melted in an EAF. The input for reducing the iron ore in this route could be 100% renewable hydrogen which would greatly decrease CO₂ emissions of the process, while the electricity provided to the EAF should come from renewable sources.

Another path for reducing the carbon intensity of this industry is to increase the rate of recycling with the use of more EAF processes. However, the potential for this solution

is limited because steel scrap is often contaminated, notably with copper, which leads to the production of lower-grade steel that is not suited for some applications, such as in the automotive industry. The use of the EAF process could therefore increase but cap at 60% to 70% of the total steel production [32].

The production technologies added to the model are therefore the following :

- H₂ DRI-EAF: Direct reduced iron with hydrogen, followed by the electric arc furnace.
- Gas DRI-EAF: Direct reduced iron with syngas, followed by the electric arc furnace.
- BF-BOF: Blast Furnace-Basic Oxygen Furnace, the traditional route using coal as a main source of energy and to reduce the iron ore.
- EAF (scrap): the secondary route using steel scrap.

3.4 Conversion technologies

Various routes for producing the necessary fuels to supply different demands coexist. Some, such as gasification from biomass to obtain methane, the Haber-Bosch process for ammonia production from hydrogen, and pyrolysis, are already present in the model. However, certain missing technologies have been incorporated.

Renewable fuel production can be based on two distinct base energy vectors: biomass and electricity. Renewable fuels produced from electricity through a Power-to-Liquid (PtL) process are referred to as electro-fuels, while those obtained from biomass are known as bio-fuels.

Another promising technology in terms of enhancing network flexibility is regenerative fuel cells. These cells allow for electricity production from hydrogen during peak consumption hours and can also produce hydrogen from surplus electricity. This technology could be a cost-effective asset for integrating intermittent energy sources on a larger scale [33]. The subsequent section briefly describes bio-fuels and electro-fuels, with a graphical summary of renewable fuel layers and conversion technologies shown in figure 3.1.

3.4.1 Bio-fuels

The European Commission recommends against supporting first-generation biofuels, which are crop-based, due to their limited scalability potential, competition with the food industry for land, and higher GHG intensity resulting from land-use change [34]. Therefore, this study focuses exclusively on second-generation bio-fuels derived from wood, biomass residue, and waste. To verify this approach, first-generation feedstocks have not been

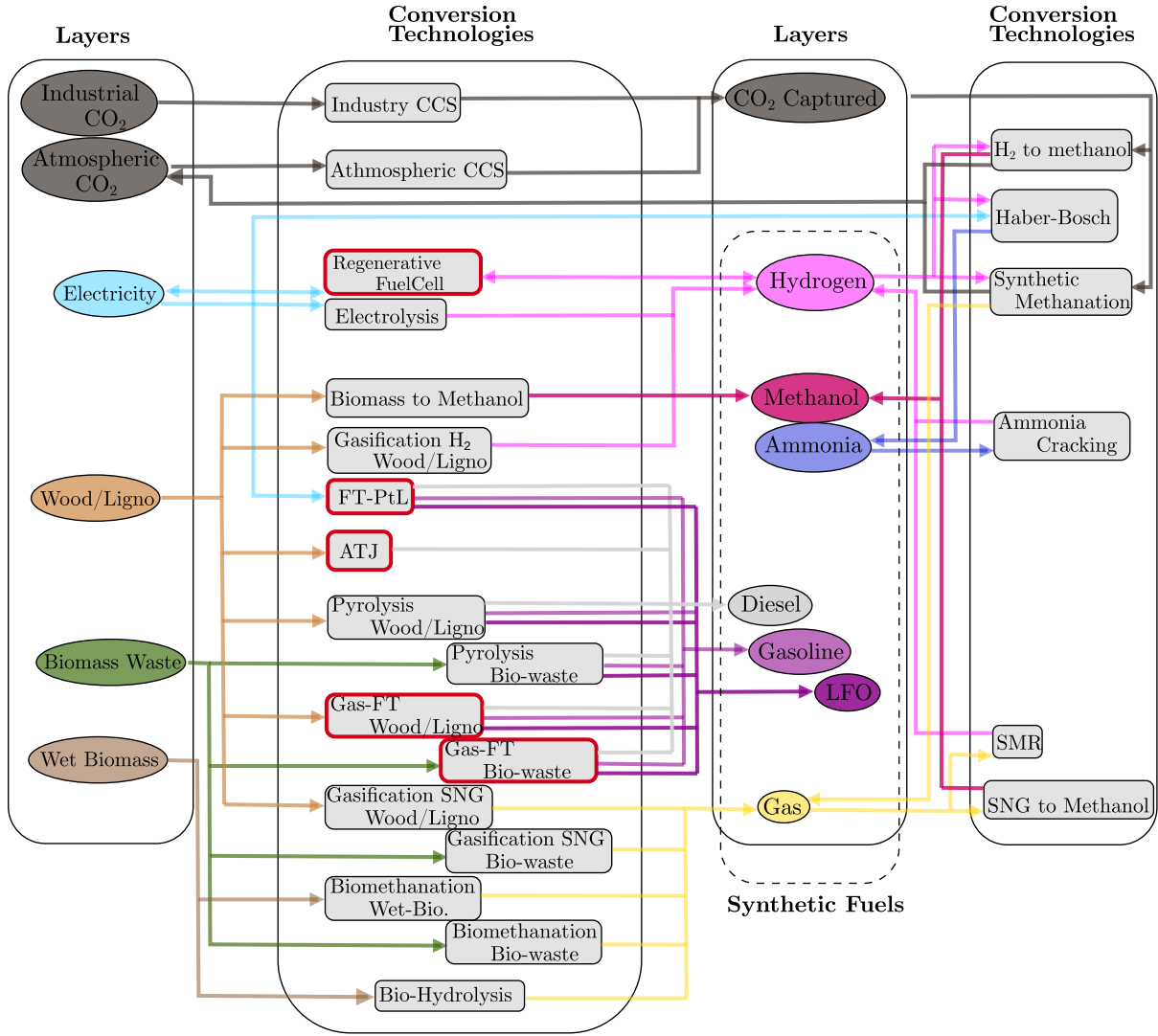


Figure 3.1: Summary of the implementation of synthetic fuels layers and related conversion technologies. Newly added technologies are highlighted in red. The figure also includes CO₂ management. Abbreviations: Steam Methane Reforming (SMR), Light Fuel Oil (LFO), Fischer-Tropsch (FT), Power to Liquid (PtL), Alcohol to Jet Fuel (AtJ), gasification + Fischer-Tropsch (gas-FT), Synthetic Natural Gas (SNG), Carbon Capture and Storage (CCS).

included in the biomass potential in the model [6].

In the literature, four processes are highlighted for biofuel production: hydro-processed esters and fatty acids synthetic paraffinic kerosene (HEFA-SPK), Alcohol-to-jet-SPK (AtJ-SPK), gasification + Fischer-Tropsch-SPK (FT-SPK), and the pyrolysis process. However, the HEFA-SPK process is excluded from the model due to the absence of the required resource in EnergyScope and its negligible potential compared to other biomass resources [35].

All these processes have received ASTM drop-in certification with a 50% blend-in, except for pyrolysis, which lacks certification. ASTM, the "American Society for Testing and Materials," sets the standard for aviation fuel certifications. Drop-in fuel derived from processes certified by ASTM can be blended with fossil jet fuel up to a certain percentage. Improvements in sustainable aviation fuel production could eventually lead to a 100% ratio for current drop-in fuel [30], explaining why limits on renewable aviation fuel blend-in percentages are not enforced in the model.

ATJ-SPK The Alcohol-to-Jet (ATJ) process for second-generation fuel production employs advanced techniques, including hydrolysis and fermentation, to generate ethanol from lignocellulosic feedstocks such as woody and grassy materials and waste. Ethanol is subsequently converted into jet fuel and middle petroleum distillates.

Gasification + FT-SPK Gasification can convert nearly any carbon-based source into syngas, a blend of carbon monoxide and hydrogen. This syngas can then be utilized in the Fischer-Tropsch process to produce fuels ranging from small-chain hydrocarbons to heavier fuels.

Pyrolysis Pyrolysis-type technologies can process a wide array of feedstocks to yield crude bio-oil by rapidly heating them to high temperatures for a few seconds. The bio-oil can then be further upgraded into higher-value fuels. While pyrolysis is commercially available, the upgrading process is still at an early demonstration stage. This process has been recently updated by ...

3.4.2 Electro-fuels

Electro-fuels are produced from electricity and CO₂ captured either from the atmosphere or from concentrated sources such as cement plants. The literature proposes two primary pathways: the Fischer-Tropsch pathway and the methanol pathway. Both are in early stages and exhibit comparable prices and efficiencies. Therefore, the model incorporates only the Fischer-Tropsch route, which already holds ASTM certification [30], unlike the

methanol pathway.

The Fischer-Tropsch pathway involves the production of syngas from hydrogen derived via water electrolysis and CO₂ obtained through atmospheric or point source capture. The syngas can then undergo regular Fischer-Tropsch processing. While breakthrough technologies like solid oxide electrolyzer technology (SOEL) and co-electrolysis promise high efficiencies, their widespread commercial availability in the near future is uncertain. Consequently, the approach in this study relies on the more traditional technologies that are the proton exchange membrane electrolyzers and CO₂ captured from concentrated sources.

3.5 Hydrogen network

Hydrogen, as an energy carrier, will need to be transported extensively from production sites to consumption or storage locations. This transportation aims to optimize production and consumption costs, as well as facilitate the integration of intermittent energy sources by connecting regions with less correlated energy production from intermittent sources [36][37]. Several transport options are considered in studies on this subject: compressed hydrogen pipelines, hydrogen shipping via ships, ammonia shipping, liquefied hydrogen shipping, and hydrogen stored in liquid organic hydrogen carriers (LOHCs) via ships. Hydrogen can also be distributed by trucks or trains to smaller consumers where required.

The transportation cost of hydrogen varies based on the mode of transport and distance traveled. Compressed hydrogen pipelines are found to be the most cost-efficient for distances less than 3000 km (the threshold can decrease to 1800 km under specific operational conditions and pipeline types)[36][37]. Given the proximity and interconnection of European Union countries, this technology is considered in this work.

This study only considers hydrogen exchanges between European countries and does not account for potential imports from North Africa or other countries, even though hydrogen costs would be lower (1€/kg compared to 1.5-2€/kg in the EU [36]). Future extensions of EnergyScope MC may include such imports, and model modifications are designed with this possibility in mind.

In addition to building new pipelines, converting existing gas pipelines into hydrogen pipelines and injecting hydrogen into the gas network are solutions considered and discussed by stakeholders [38] [39]. These solutions are incorporated in this work, and their impact on the system will be analyzed.

Modeling the hydrogen network serves three main purposes. First, it offers a more accurate representation of hydrogen as an energy carrier’s cost. Second, it enables the analysis of the positive or neutral impact of a hydrogen network on system costs. Finally, it helps determine optimal hydrogen exchange capacities between countries and the proportion of repurposed gas pipelines. In future studies, it can also facilitate a comparison of hydrogen transportation methods for imports from Northern African countries.

3.5.1 Model Philosophy

For the results to be meaningful, the model should consider the entire cost of transporting hydrogen across the modeled regions. Hydrogen pipelines are necessary not only for international exchanges, transferring hydrogen from cheaper production countries to consumption countries, but also for domestic transportation within a country, from production sites to consumption sites. While domestic infrastructure will eventually be used to distribute energy imports locally, it should not bear the full cost of the entire system, and vice versa. Thus, considering the cost of domestic networks and international exchanges separately is natural.

An observation by Cornet N. and Eloy P. in [15] is that energy transfer may not only occur between pairs of neighboring countries but may also be exported and transit through other countries before reaching the final destination. However, in EnergyScope, interconnection costs are only considered for short interconnections for gas [14] and for 130 km lines for electricity [15]. This becomes problematic because the cost of reinforcing local grids, whether for electricity or gas, is not included in the current model version. Consequently, energy exchange prices in the model are lower than in reality. This issue has also been noted by [15]: *"... introducing long-distance interconnections has some limitations with the current implementation of the model. Indeed, the cost to reinforce the local grid is not taken into account for regions that import electricity. The cost to connect two cells by means of one intermediate is then lower than building a long line between the two furthest cells."*

In this work, another issue arises due to the current implementation. The optimal capacity of repurposed hydrogen pipelines results from a trade-off between the cost benefits of repurposing pipelines (36% of the cost of new pipelines, based on table 4.12) and the constraint of limiting gas exchange capacity. However, using short interconnection lengths limits the economic advantages of repurposed hydrogen pipelines, under the same gas exchange capacity constraint. Consequently, there is little incentive to convert gas pipelines to hydrogen pipelines. Moreover, this also highlights a potential bias favoring pipeline routes over shipping routes in future comparisons of hydrogen transportation from North Africa.

For these reasons, the decision has been made to update energy exchange costs for gas, electricity, and hydrogen. These costs now reflect network reinforcement costs more accurately. The costs are based on interconnection lengths between countries in the EHB 2040 map [40]. The interconnections considered are illustrated in figure 3.2 (see section 4.5.1 for exact start and end points of each interconnection). While this approach seems more natural for hydrogen, given the need to build the entire backbone, it is a simplified approximation for electricity and gas. Constructing new short interconnections and accounting for domestic grid reinforcement could potentially result in lower costs than connections spanning a significant portion of a country. For further details on how these costs and costs of domestic hydrogen networks are calculated, refer to sections 4.5.1 and 4.5.2.

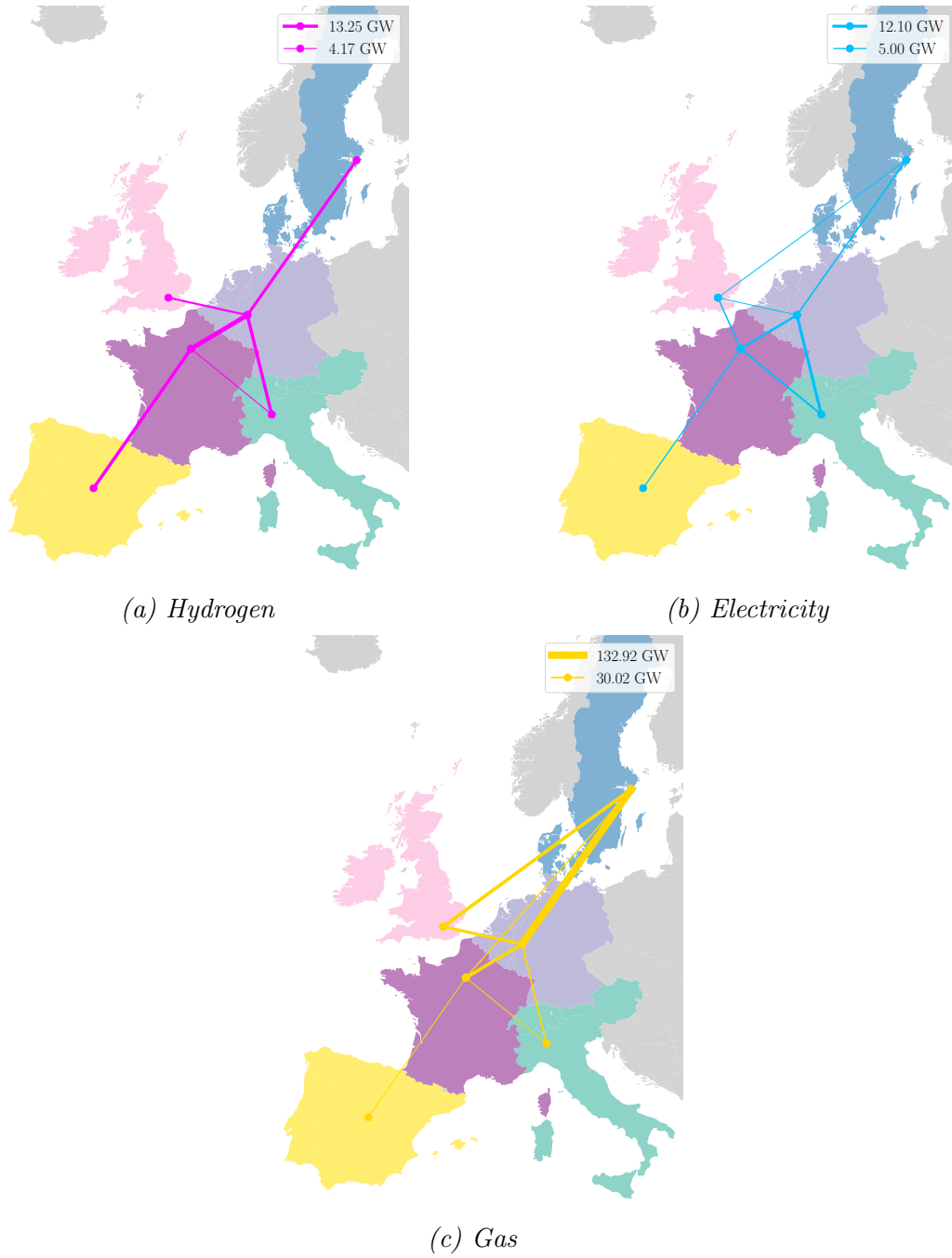


Figure 3.2: Interconnection patterns for the three exchange networks considered in the model.

3.5.2 Practical implementation in EnergyScope MC

This section details the constraints added to the AMPL code and the constraints modified used to model the energy exchanges. Some variables are created and the syntax is simplified to ease the understanding.

Eq. 3.1 limits the variable *TransferCapacity* between maximum and minimum bounds. The parameter tc_{mul} is a multiplication factor used to multiply the reference maximum bound tc_{max} .

$$\begin{aligned} \forall c_1 \in \text{REGIONS}, c_2 \in \text{REGIONS}, i \in \text{EXCH_NTW} - \{\text{"GAS"}\} \\ tc_{min}^{c_1, c_2, i} \leq \text{TransferCapacity}^{c_1, c_2, i} \leq tc_{mul}^i \cdot tc_{max}^{c_1, c_2, i} \end{aligned} \quad (3.1)$$

Eq. 3.2 relates the fact that the transfer capacity plus the "will be converted" transfer capacity of gas pipeline must be between the maximum and minimum bounds. As explained in section 4.5.1, these bounds are really tight (almost a single value) and correspond to the capacity of the ten year development plan of the ENTSG.

$$\begin{aligned} \forall c_1 \in \text{REGIONS}, c_2 \in \text{REGIONS} \\ tc_{min}^{c_1, c_2, \text{"GAS"}} \leq \text{TransferCapacity}^{c_1, c_2, \text{"GAS"}} + \text{TotalConvCapacity}^{c_1, c_2} \leq tc_{mul}^{\text{"GAS"}} \cdot tc_{max}^{c_1, c_2, \text{"GAS"}} \end{aligned} \quad (3.2)$$

Eq. 3.3 and Eq. 3.4 constrains the total converted capacity of gas pipeline. The first one is activated when hydrogen exchange is allowed while the second is activated otherwise. When hydrogen exchange is enabled, the hydrogen capacity coming from repurposed gas pipeline should be smaller than the total hydrogen exchange capacity. If no hydrogen exchange is allowed, then the converted capacity should be zero.

$$\begin{aligned} \forall c_1 \in \text{REGIONS}, c_2 \in \text{REGIONS} \\ (1 - \text{capacityLoss}_{H2_ntw}) \cdot \text{TotalConvCapacity}^{c_1, c_2} \\ \leq \text{conv}_{max} \cdot \text{TransferCapacity}^{c_1, c_2, \text{"H2"}} \end{aligned} \quad (3.3)$$

or

$$\text{TotalConvCapacity}^{c_1, c_2} \leq 0 \quad (3.4)$$

Eq. 3.5, 3.6 and 3.7 evaluate the cost of the networks when hydrogen exchange is allowed. Note that Eq.3.6 is only valid when tight bounds are used on the gas transfer capacity and it stipulates that all the available pipeline capacity is built. Indeed, this capacity should be built before it can possibly be converted to hydrogen pipelines. 3.7 states that the whole cost is paid for the hydrogen pipeline capacity that does not come from the repurposed gas pipeline, while a reduced cost is paid for the repurposed capacity. Note that these costs are given per unit of hydrogen capacity.

$$\begin{aligned} \forall c \in \text{REGIONS}, i \in \text{EXCH_NTW} - \{\text{"GAS"}, \text{"H2"}\} \\ \text{Cost}_{ntw}^{c, i} = \sum_{c_2 \in \text{REGIONS}} \text{cost}_{ntw}^{c, c_2, i} \cdot \text{TransferCapacity}^{c, c_2, i}. \end{aligned} \quad (3.5)$$

$\forall c \in \text{REGIONS}$

$$Cost_{ntw}^{c, "GAS"} = \sum_{c_2 \in \text{REGIONS}} cost_{ntw}^{c, c_2, "GAS"} \cdot tc_{max}^{c, c_2, "GAS"} \quad (3.6)$$

$\forall c \in \text{REGIONS}$

$$\begin{aligned} Cost_ntw^{c, "H2"} &= \sum_{c_2 \in \text{REGIONS}} cost_{ntw}^{c, c_2, "H2"} \cdot (TransferCapacity^{c, c_2, i} \\ &- (1 - capacityLoss_{H2_ntw}) \cdot TotalConvCapacity^{c, c_2}) \\ &+ cost_{repurpose}^{c, c_2} \cdot (1 - capacityLoss_{H2_ntw}) \cdot TotalConvCapacity^{c, c_2} \end{aligned} \quad (3.7)$$

Eq. 3.8 already existed in the code and is still used to compute the exchange costs when hydrogen exchange is not considered.

$\forall c \in \text{REGIONS}, i \in \text{EXCH_NTW}$

$$Cost_{ntw}^{c, i} = \sum_{c_2 \in \text{REGIONS}} cost_{ntw}^{c, c_2, i} \cdot TransferCapacity^{c, c_2, i}. \quad (3.8)$$

Eq. 3.9 states that the quantity of hydrogen injected in the network at a certain time should not be above a fixed ratio of the gas produced at that instant.

$\forall c \in \text{REGIONS}, h \in \text{HOURS}, td \in \text{TD}$

$$H2_{inj}^{c, h, td} \leq injectionRatio_{max} \cdot Gas_{prod}^{c, h, td} \quad (3.9)$$

Eq. 3.10 gives the installed capacity of the domestic hydrogen network in GW. This capacity is proportional to the hydrogen circulating in the country, which is estimated by taking the mean of the demand and supply of hydrogen. The network is used with a load factor expressed in hour per year $loadHour_{H2_grid}$. Eq. 3.11 states that the installed power of the compressors is the same as the one for the pipelines (price is calculated accordingly).

$\forall c \in \text{REGIONS}$

$$F^{c, "H2_PIPELINE"} = \frac{H2_{prod}^c + H2_{cons}^c}{2 \cdot loadHour_{H2_grid}} \quad (3.10)$$

$$F^{c, "H2_COMPRESSOR"} = F^{c, "H2_PIPELINE"} \quad (3.11)$$

parameters

- $tc_{min}^{c_1, c_2, i}$: minimum transfer capacity in GW for the resources i from the region c_1 to the region c_2 .
- tc_{mul}^i : multiplication factor for the maximum transfer capacity of resource i . This factor is 1 for gas and 2 for electricity and hydrogen.
- $tc_{min}^{c_1, c_2, i}$: maximum transfer capacity in [GW] for the resources i from the region c_1 to the region c_2 .
- $conv_{max}$: maximum ratio of capacity obtained from repurposed gas pipeline over transfer capacity. Can be put to 0 in case no conversion is desired.
- $cost_{ntw}^{c, c_2, i}$: total cost of the network in M€/GW/year for resource i , from region c to regions c_2 .
- $cost_{repurpose}^{c, c_2}$: total cost for repurposing gas pipelines into hydrogen ones in M€/GW_{H₂}/year, for transfer from region c to region c_2 .
- $injectionRatio_{max}$: maximum injection ratio of hydrogen into the gas network.
- $capacityLoss_{H_2 ntw}$: ratio of capacity loss when converting a unit capacity of gas pipeline into hydrogen pipeline.
- $loadHour_{H_2 grid}$: Load factor of the hydrogen network in hours per year.

Variables

- $TransferCapacity^{c_1, c_2, i}$: Transfer capacity for resource i , from region c_1 to region c_2 .
- $TotalConvCapacity^{c_1, c_2}$: Total gas capacity converted to the benefit of hydrogen exchange capacity, for transfer from region c_1 to region c_2 .
- $cost_{ntw}^{c, i}$: Total cost of the networks exporting resource i from region c .
- $H2_{inj}^{c, h, td}$: Quantity of hydrogen injected into the gas network, at hour h of the typical day td , in the region c .
- $Gas_{prod}^{c, h, td}$: Quantity of gas produced or imported from the exterior of the global system in the region c , at hour h of the typical day td .
- $F^{c, j}$: Installed capacity in GW of technologies j in regions c .
- $H2_{prod/cons}$: Annual production/consumption of hydrogen in region c .

SETS

- REGIONS: The set of all the regions modeled.
- EXCH_NTW: The set of resources that can be exchanged via a network.
- HOURS: The hours of the day.
- TD: The set of all the chosen typical days.

Chapter 4

Data collection

4.1 International shipping

4.1.1 Demand

Demand for international shipping was evaluated for every country in the European Union plus Switzerland - whose demand is null - in view of the future use of the model for the entire European energy system. The results of the EU reference scenario 2020¹ are used to determine the international shipping demand "*Int.Maritime*". However, as these data are not directly available in the scenario results, some manipulations are necessary to obtain them. The data available are first the total energy demand for freight transportation "*Total Freight Demand*" in kiloton of oil equivalent (ktoe). These data include international intra and extra-EU maritime freight transportation. Other available data are the energy intensity of freight transportation "*Freight Energy Intensity*" in toe/Mt-km and road "*Road Freight*", rail "*Rail Freight*" and inland maritime "*Inland Maritime*" freight transportation activities in Gt-km. The steps for obtaining the relevant data are then the following:

$$Total\ Freight\ Demand\ [Gt-km] = \frac{Total\ Freight\ Demand\ [ktoe]}{Freight\ Energy\ Intensity\ [ktoe/Gt-km]},$$

gives the total freight demand accounting for international maritime.

$$Int.\ Maritime\ [Gt-km] = Total\ Freight\ Demand\ [Gt-km] - \\ (Road\ Freight + Rail\ Freight + Inland\ Maritime)\ [Gt-km],$$

gives the required data.

However, data were not available for the United Kingdom. A ratio between the gross weight of goods handled in main port "*Gross Weight*"² in France and the UK was used to estimate the total freight demand in Gt-km in the following way:

$$Int. Maritime_{UK} [Gt\cdot km] = \frac{Gross Weight_{UK}}{Gross Weight_{FR}} Int. Maritime_{FR} [Gt\cdot km],$$

resulting from the assumption that France and the UK have similar international commercial partners.

[41] defines the data collected and used in the PRIMES-TREMOVE model (used to provide the reference scenario data) like this: *"By assumption, 50% of the calculated transport performance is allocated to the origin country and 50% to the destination country. The same "50%-50%" principle allocation applies to the EFTA countries and the candidate countries. For the international extra-EU activity, where the corresponding partner is outside EU-28 and is not an EFTA or candidate country, 100% of transport performance is allocated to the declaring EU MS country"*. Assuming that the transport performance refers to the total gross weight of goods handled in the country, it is concluded that for extra-EU maritime transport, demand might be twice as large as it should be when it comes to refueling the ships. However, this is if the said reports concern incoming and outgoing ships, which is unclear. Also, sharing the demand between the partners in two means that the receiving country shares a part of this demand, even though it did not contribute to refueling the ship. However, due to a lack of other data sources, these data are considered satisfying. A graphical representation of the demand is presented in figure 4.1

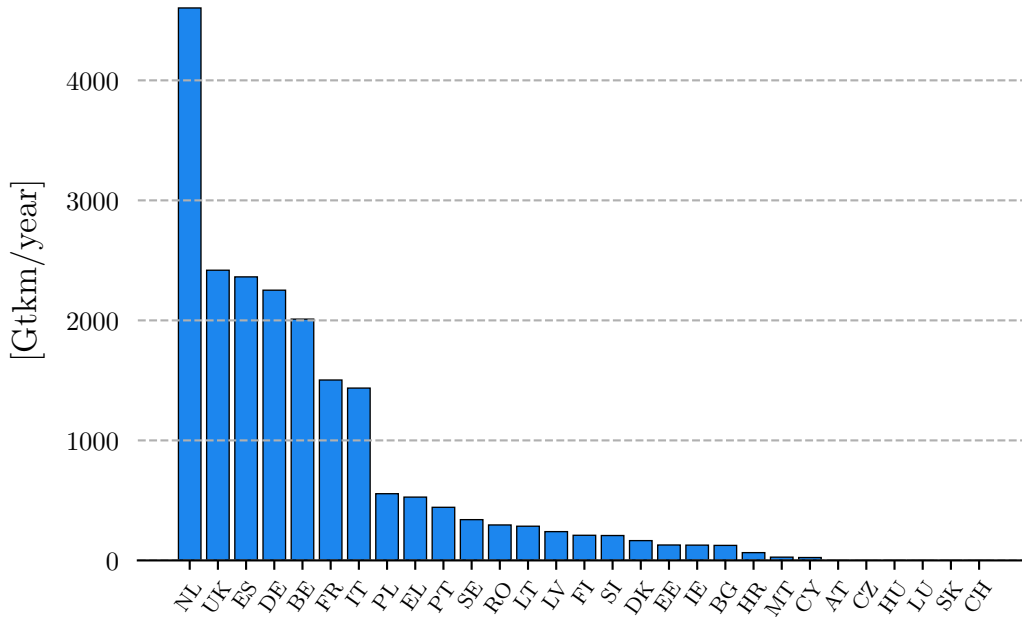


Figure 4.1: Projected EU international maritime freight demand per country for the year 2035, in Gt·km/year.

4.1.2 Technologies

This section presents the model parameters for maritime technologies, their sources, and the methodology to obtain them. Intermediate parameters used to evaluate model parameters are also shown, as well as their sources and the methodology to obtain them. Model parameters are grayed in the tables.

Av. distance ³ [1000km/y]	Av. speed ⁴ [km/h]	Lifetime ⁵ [y]	c_p ⁶ [-]	Tonnage ⁷ [t/ship]	TEU Capacity ⁸ [TEU/ship]	TEU Load ⁹ [t/TEU]
288	42.6	25	0.77	56000	4000	14000

Table 4.1: Parameters common to all cargo shipping technologies implemented in the model (Tonnage is different for retrofitted ammonia and methanol ships).

Cargo type	c_{inv} ^{1.} [€/t-km/h]	c_{maint} ^{2.} [€/t-km/h/y]	Ship Capacity ^{3.} [kt-km/h/veh.]	Fuel Cons. ^{4.} [Wh/t-km]		
				Total	Main	Pilot
Fuel Oil	18.67	1.85	2385	23.8	-	-
LNG	21.66	2.15	2385	21.97	-	-
Methanol (ICE)	20.73	2.06	2385	23.8	22.62	1.19
Ammonia (ICE)	21.66	2.15	2385	22.88	23.81	1.99
Ammonia (FC)	26.92	2.68	2385	18.2	-	-
LH2 (FC)	26.92	2.68	2385	20.52	-	-
Methanol retro.	3.11	2.15	2290	24.8	23.57	1.24
Ammonia retro.	4.84	2.32	2211	25.68	23.63	2.06

Table 4.2: Costs, shipping capacities, and fuel consumptions of the implemented shipping technologies.

4.1.3 Sources and methodologies

Reference	Methodology	Source
1.	-	EU Reference Scenario 2020: Summary report: Energy, transport, and GHG emissions.
2.	-	Eurostat data code : MAR_MG_AM_CWHC
3.	-	https://www.ioscm.com/blog/industry-facts-101-the-shipping-industry-is-enormous/
4.	-	<i>Second IMO study 2009</i> , p.131.
5.	-	[18], p.77.
6.	Calculated in the following way : $c_p = \frac{Av. distance}{Av. speed \cdot 8760}$	-
7.	TEU load is multiplied by the TEU capacity. For ammonia and methanol ships reconverted from oil ships, the ratio of container space loss over TEU capacity following the conversion (1) is used to reevaluate the Tonnage.	(1) [18]
8.	The average capacity of container ships is 3420 TEU/ship. The closest standard size for a container ship was then 4000 TEU/ship.	UNCTAD : <i>Escales et données sur la performance</i> emph : temps passé dans les ports, âge et taille des navires, annuel.
9.	Maximum allowable weight per TEU (1) is multiplied by the number of TEU per ship and by the Average yearly capacity utilization (2).	(1) https://www.ukpandi.com/news-and-resources/bulletins/2021/overweight-container-guide/ . (2) <i>Second IMO study 2009</i> , p.131.

Table 4.3: Sources and methodologies for international maritime freight demand and technologies.

4.2 Aviation

4.2.1 Demand

Data for aviation demand are compiled differently than for international maritime demand. The reference scenario 2020 is not used, firstly because extra-EU demand data are not available, and secondly because of the quality of the data when it comes to fuel calculation, as mentioned in section 4.1.1. Data from Eurostat are considered a better source and provide data for intra-EU and extra-EU aviation. The data taken are the number of passengers between pair of countries, from EU countries to extra-EU countries¹

and between EU countries 2, for the year 2019 (before COVID). The subset of the data considered is "PAS_CRD_DEP", as it contains the number of passengers embarking on the plane that takes off from the reporting EU country. The python package *geopy* is then used to create a distance matrix containing the distance between each pair of countries, allowing to adapt Eurostat data and obtain them in Gp-km. Finally, the rates of country-specific aviation demand increase provided by Eurocontrol 3 and summarized in table C.3 are used to project the demand to 2035.

Data for Switzerland are not available in the data set. To estimate them, a population-weighted average of the demand was performed on the data for Austria. A summary of the data is available for visualization in figure 4.2.

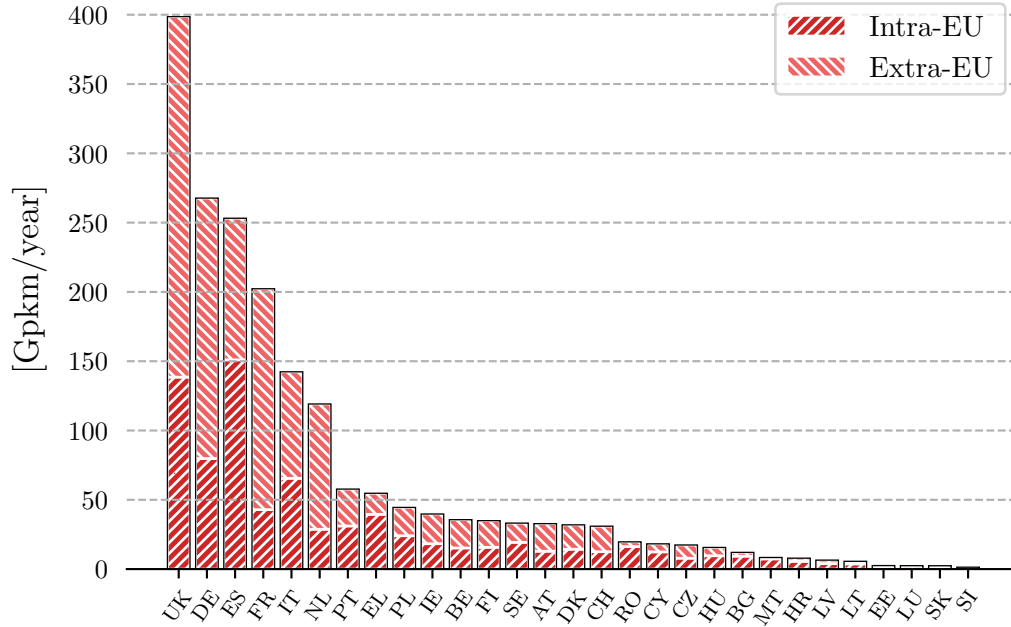


Figure 4.2: Projected EU aviation demand for 2035, in Gpkm/year. Extra-EU demand refers to flights landing in a country that is not part of the EU (2019). Intra-EU demand refers to flight landing in an EU country (2019). A flight is accounted for in the country in which it takes off.

4.2.2 Technologies

This section presents the model parameters for aviation technologies, their sources, and the methodology to obtain them. Intermediate parameters used to evaluate model parameters are also shown, as well as their sources and the methodology to obtain them. Model parameters are grayed in the tables.

Ref. aircraft	c_{inv}^4 [€/p-km/h]	c_{maint}^5 [€/p-km/h/y]	c_p^6 [-]	Fuel Cons. ⁷ [Wh/p-km]
Airbus A320	1456	39.82	0.5	263.5
Boeing 777	1343	36.75	0.53	419.79
Narrow-body H ₂	1639	44.84	0.5	368.72
	Av. speed ⁸ [km/h]	Aircraft capa. ⁹ [kp-km/h/veh.]	Lifetime ¹⁰ [y]	Occupancy ¹¹ [pass/veh.]
Airbus A320	498	76.2	35	153
Boeing 777	824	238	35	289
Narrow-body H ₂	498	76.2	35	153

Table 4.4: Main model parameters and intermediate parameters for the implemented aviation technologies.

4.2.3 Sources and methodology

Ref.	Methodology	Source
1.	-	Eurostat code : avia_paincc
2.	-	Eurostat code : avia_paexcc
3.	-	[31], figure 5
4.	Data for the A320 and the Boeing 777 are taken from (1). The additional cost for hydrogen-fueled gas turbines planes is taken from (2). The data are modified to fit the model units :	(1) http://www.axonaviation.com/commercial-aircraft/aircraft-data/aircraft-pricing . (2) [29]. p.140.
	$c_{inv} = \frac{\text{Plane cost}}{\text{Occupancy} \cdot \text{Av. speed}}$	
5.	Maintenance cost is determined for the A320. The same ratio of maintenance cost over investment cost is then applied to the Boeing 777 and the hydrogen plane. Finally, the costs are put in the right units as for the investment cost.	https://aviatorinsider.com/airplane-brands/airbus-a320/

6.	Utilization rates are taken for the A320 and Boeing 777. Note that these are just estimates because the utilization rates vary widely with flight companies.	https://blog.gitnux.com/aircraft-utilization-statistics/
7.	Average flight lengths for intra and extra EU flights are computed with a Python program using Geopy and the data from Eurostat (2,3), and are equal to 1350 km and 4500 km. The reference flight for intra and extra EU flights chosen from the study (1) are then respectively the flights <i>LHR-MAD A320</i> (1244km) and <i>LHR-JFK 777</i> (5539km), and their consumption in kWh/km is finally retrieved.	(1) https://www.oag.com/blog/which-part-flight-uses-most-fuel . (2) Eurostat code : via_paincc . (3) Eurostat code : avia_paexcc.
8.	Representative flights are taken and their speed is calculated (based on block hours).	(1) https://www.ryanair.com . (2) https://www.brusselsairlines.com .
9.	Aircraft capacity is evaluated in the following way, to fit the model units : $Plane\ capa. = Occupancy \cdot Av. speed$	-
10.	-	https://simpleflying.com/how-many-engines-do-airliners-go-through/
11.	Data on seats available are taken from (1) and (2). They are then multiplied by the passenger load factor, taken from (3).	(1) https://aviatorinsider.com/airplane-brands/airbus-a320/ . (2) https://www.boeing.com/farnborough2014/pdf/BCA/bck-777%20Family%20Backgrounder.pdf . (3) IATA : air passenger analysis, August 2022.

Table 4.5: Sources and methodologies for aviation demand and technologies.

4.3 Steel

4.3.1 Demand

Steel production by country is taken from the European steel association¹. For countries that do not appear in the publication (CY, DK, EE, IE, LT, LV, MT, PT, UK, CH), their steel production is taken from the World steel association². The data are not projected to 2035 and it is seen as a model improvement.

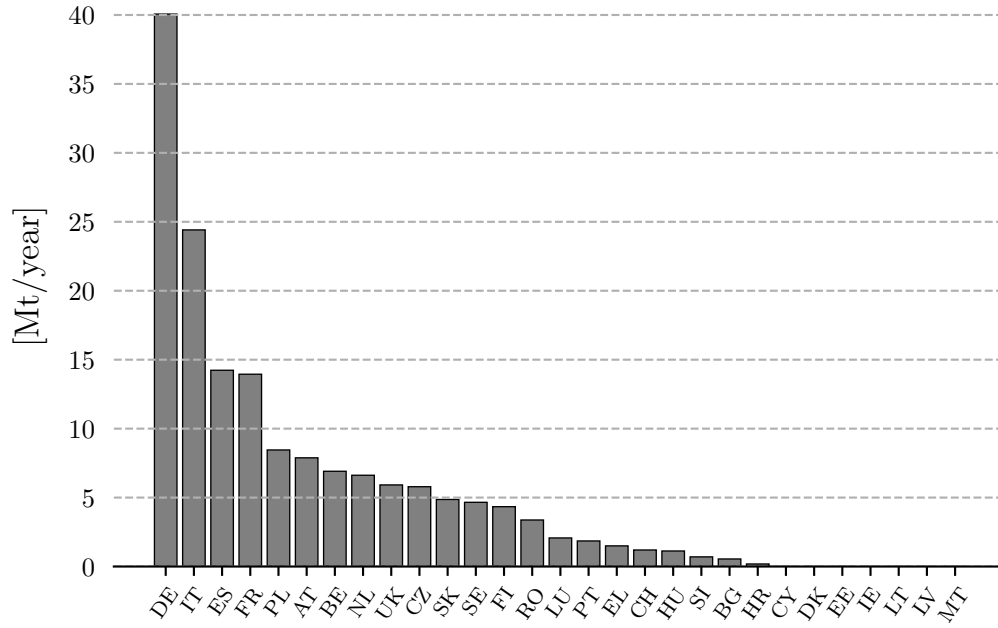


Figure 4.3: European steel production per country in 2021, in Mt/year.

4.3.2 Technologies

Process	Hydrogen [GWh/kt]	Electricity [GWh/kt]	Coal [GWh/kt]	Gas [GWh/kt]	Total [GWh/kt]
H2 DRI-EAF	1.83 ³	0.93 ³	0.09	-	2.76
Gas DRI-EAF	-	0.83 ³	-	2.78 ³	3.61 ³
BF-BOF	-	0.41 ⁴	5.19 ⁴	0.23 ⁴	5.83 ³
EAF (scrap)	-	0.74 ³	0.09 ³	-	0.83 ³

Table 4.6: Inputs and outputs of the different production routes considered for steel making.

Data from table 4.6 are not exactly the same as the ones put in the model. Indeed, it is considered that the carbon source -coal for now- necessary for the carburization of the steel and the slag foaming production in the EAF can be provided by biochar [42]. The production of the biochar is however not implemented in the model.

Process	c_{inv}^5 [M€/kt/h]	c_{maint}^5 [M€/kt/h/year]	Lifetime ⁶ [years]	C_p [-]
H2 DRI-EAF	5641	282	40	1
Gas DRI-EAF	5641	282	40	1
BF-BOF	6447	322	40	1
EAF (scrap)	4030	201	40	1

Table 4.7: Main model parameters for the different routes considered for steel production.

4.3.3 Sources and methodologies

Ref.	Methodology	Source
1.	-	Eurofer : <i>European steel in figures 2022</i> .
2.	-	https://worldsteel.org/steel-topics/statistics/annual-production-steel-data/?ind=P1_crude_steel_total_pub/CHN/IND .
3.	-	[32]
4.	-	World Steel Association : <i>Fact sheet : Energy use in the steel industry</i> .
5.	Price is taken from the source, excluding the electrolyzer price. O&M cost is assumed to be 5%.	https://sustainability.crugroup.com/article/the-cost-of-decarbonising-european-steel-is-high
6.	-	IEA : <i>Average age and typical lifetime of assets in the iron and steel and cement industries, China</i>

Table 4.8: Sources and methodologies for steel supply and production technologies.

4.4 Conversion technologies

Technology	c_{inv} [M€/GW _{in}]	c_{maint} [M€/GW _{in}]	c_p [-]	Lifetime [years]
FT (PtL) ¹	975	49	0.93	25
ATJ-SPK ¹	851	42	0.96	25
Bio FT-SPK ¹	1028	31	0.91	25
Regen. FC ²	873	26	0.9	15

Table 4.9: Main parameters for the conversion technologies implemented in the model.

Technology	Biomass [GWh]	Electricity [GWh]	Gasoline [GWh]	Diesel [GWh]	LFO [GWh]	CO ₂ [kt]	DHN [GWh]
FT (PtL) (Gasoline)	0	-1	0.45	0	0	-0.141	0.2
FT (PtL) (Diesel)	0	-1	0.112	0.338	0	-0.141	0.2
FT (PtL) (LFO)	0	-1	0	0.112	0.338	-0.141	0.2
Bio FT-SPK (Gasoline)	-1	0	0.274	0	0	0	0.376
Bio FT-SPK (Diesel)	-1	0	0.068	0.205	0	0	0.376
Bio FT-SPK (LFO)	-1	0	0	0.068	0.205	0	0.376
ATJ-SPK	-1	0.006	0	0.293	0.007	0	0

Table 4.10: Input and output for the conversion technologies implemented in the model.¹

Concerning regenerative fuel cells, their conversion efficiency in electrolysis mode is 80% while it is 65% in fuel cell mode².

Ref.	Methodology	Source
1.	<p>Data for FT (PtL) and Bio FT-SPK are taken from (1). A linear interpolation is performed since data are only available for the years 2030 and 2040. Note that a continuous range of operation is possible for Fischer-Tropsch processes, producing different proportions of each class of distillates. Also, hydrocracking is possible downstream of the process to convert long-chain hydrocarbons into lighter distillates. Following data from (1) and (2), the proportions put in the table above are chosen as representative ones. Data for the ATJ-SPK process are taken from (3), for switchgrass. It should be noted that the ATJ-SPK process also requires 0.07 GWh of natural gas. To evaluate the available heat for DHN in the Fischer-Tropsch processes, the process heat loss was assumed to be 35%.</p>	<p>(1) Danish Energy Agency: <i>Technology descriptions and projections for long-term energy planning: Renewable fuels</i>.</p> <p>(2) Mahdi Fasihi, Dmitrii Bogdanov, Christian Breyer : <i>Techno-Economic Assessment of Power-to-Liquids (PtL) Fuels Production and Global Trading Based on Hybrid PV-Wind Power Plants</i>. Table 6.</p> <p>(3) Guolin Yao, Mark D. Staples, Robert Malina, and Wallace E. Tyner: <i>Stochastic techno-economic analysis of alcohol-to-jet fuel production</i>. Table 3.</p>

-
2. All the data are taken from the article, except the availability, which is taken the same as the one for the electrolyser already implemented in the model. The investment price is deduced for 2035 using a price decrease of 7% per year, which is in the conservative part of the range given in the paper. The efficiencies are the ones projected for 2030. [33], Table 1.

Table 4.11: Sources and methodologies for conversion technologies characteristics.

4.5 Networks

4.5.1 Exchange networks

Other parameters than the ones in the following tables are used in the networks modeling (they are defined in section 3.5.2:

- *inj_ratio_max*: is set to 5%. This is motivated by the fact that a vast majority of gas technologies can still be used without modification with this ratio of hydrogen¹.
- *ntw_H2_capa_loss*: the parameter can vary from 38% to 20% if considering the cost-optimal operation of the hydrogen pipeline or not². However, the optimization problem behind this is not resolved in this work and the parameter is set to 30%.
- *H2_grid_load_hour*: is set to 5000 hours³.

From/To ⁴	To/From ⁴	Length ⁵	Cost new ⁶ [M€/GW/year]	Cost repurpose ⁶ [M€/GW/year]
AT-CH-IT Milan (1)	BE-DE-LU-NL Cologne	635	16.69	5.97
AT-CH-IT Milan (2)	FR Paris	641	16.85	6.02
BE-DE-LU-NL Hamburg (3)	DK-SE Stockholm	806	21.19	7.57
BE-DE-LU-NL Cologne (4)	IE-UK Norwich	218 + 264	16.68	5.96
BE-DE-LU-NL Cologne (5)	FR Paris	409	10.75	3.84
DK-SE Esbjerk (6)	FR Paris	710 + 235	37.91	13.55
DK-SE Stockholm (7)	IE-UK Norwich	1264	56.49	20.19
ES-PT Madrid(8)	FR Paris	1054	27.71	9.9
FR Paris (9)	IE-UK London	105 + 230	10.74	3.84

Table 4.12: Costs and geographic characteristics of the hydrogen pipelines considered in the model, for new and repurposed pipelines. When two lengths are given, the first one corresponds to undersea pipelines.

Region Pair	Electricity ⁷ [M€/GW/year]	Gas ⁸ [M€/GW/year]
(1)	67.8	12.84
(2)	68.4	12.96
(3)	84.79	16.3
(4)	84.84	12.83
(5)	45.37	8.27
(6)	-	29.16
(7)	168.89	43.45
(8)	109.41	21.31
(9)	64.86	8.26

Table 4.13: Economic parameters for the gas and electricity exchange networks.

From	To	Capacity [GW]
AT-CH-IT	BE-DE-LU-NL	13.25
AT-CH-IT	FR	4.17
BE-DE-LU-NL	AT-CH-IT	13.25
BE-DE-LU-NL	DK-S	12.08
BE-DE-LU-NL	FR	18.45
BE-DE-LU-NL	IE-UK	8.33
DK-SE	BE-DE-LU-NL	12.08
DK-SE	FR	0
DK-SE	IE-UK	0
ES-PT	FR	9
FR	AT-CH-IT	4.17
FR	BE-DE-LU-NL	18.45
FR	ES-PT	9
IE-UK	BE-DE-LU-NL	8.33

Table 4.14: Maximum capacities of reference for hydrogen interconnections between countries, in GW⁹.

4.5.2 Domestic network

	Pipelines	Compressors
CAPEX [M€/GW]	196.1	66.26
OPEX [M€/GW/year]	3.15	2.01
Lifetime [years]	40	25

Table 4.15: Economic parameters for the domestic hydrogen network.¹⁰

4.5.3 Sources and methodology

Ref.	Methodology	Source
1.	-	ENTSO-G : <i>How to transport and store hydrogen - Facts and figures.</i> p.4.
2.	-	EHB report 2020 : <i>How a dedicated hydrogen infrastructure can be created.</i> p.10.
3.	-	EHB report 2021 :[39]. p.14.

4.	Cities have been chosen to represent in the best way possible the future projected network in (1), but also to represent the compromise between domestic and exchange costs.	(1) Map of the 2040 hydrogen network: <i>EHB 2022 report</i> [40], p.13.
5.	Distances are taken as straight lines. If two distances are provided in the table, the first one refers to offshore infrastructure.	https://www.google.com/maps
6.	<p>CAPEX per km for new and repurposed pipelines of 13 GW capacities are taken from (1) (summarized in table C.2). The OPEX is given in percent of the CAPEX for compressors and pipelines independently in (2) (Also summarized in table C.2). However, the total OPEX -the sum of the compressor and pipeline OPEX- calculated in this way leads to an operation and maintenance cost for the European hydrogen network that is below the projected price of the EHB in (2) (€1.6-€3.2 billion). For consistency, the total OPEX per km for the interconnections is therefore obtained by taking an OPEX of €1.8 billion for the entire network and dividing it by the total length of the hydrogen backbone (53000km (2)). As the 13 GW pipelines are projected to have the highest OPEX per km, this method probably underestimates slightly the interconnection pipelines' OPEX. The CAPEX for pipelines is divided by 13 to obtain a CAPEX per GW per km. The costs are then multiplied by the length of the interconnection, and adding a factor of 1.7 (2) for the offshore pipeline sections. Finally, the costs are annualized using a discount rate of 7.5%.</p>	<p>(1) <i>EHB 2021 report</i> [39], p.17. (2) <i>EHB 2022 report</i> [40].</p>
7.	<p>Prices for electric cables are taken from (1). One station is considered per line of 1 GW. The costs, taking into account undersea cable sections, are then multiplied by the length of the line given in table 4.12 and annualized , taking a discount rate of 7.5%.</p>	(1) International Energy Agency. <i>The Power of Transformation</i> . 2014, p.124.

8.	The total price for gas pipelines is taken as 77% of the total price for new hydrogen pipelines.	(1) EHB : <i>How a dedicated hydrogen infrastructure can be created.</i> 2020, p.19.
9.	Projected capacities for 2040 are aggregated per regions. Note that these capacities will be multiplied by the factor tc_{mul} defined in section 3.5.2.	ENTSO-G, <i>Ten year development plan, Annex C.2-H2 capacities per country.</i>
10.	<p>Prices are taken from (1) and summarized in table C.2.</p> <p>A single CAPEX per kilometer is obtained by average using the weights for the different types of pipelines.</p> <p>The OPEX per kilometer is obtained by dividing the projected price of €1.8 billion (2) by the length of the EU network (53000km). This price is then multiplied by the length of the domestic network (53000 km - total length of the H₂ interconnections).</p> <p>According to (2), the network will be sufficient to satisfy the European demand forecast of 1640 TWh, operating with a load factor of 5000 hours. The price per GW of network is therefore:</p> $CAPEX_{/GW} = \frac{CAPEX_{tot}}{1640 \cdot 10^3 / 5000}$ <p>Note, as a reminder of section 3.5.2 that the network installed quantity in GW will be:</p> $F = \frac{H_2 \text{ demand} + H_2 \text{ production}}{2 \cdot 5000}$ <p>, where the average of the demand and production in GWh is used. This is because countries that are exporting hydrogen will need a stronger network, just as much as the importing countries.</p>	<p>(1) EHB report [39]. 2021. p.17.</p> <p>(2) EHB report [40]. 2022. p.11, p.15.</p>

Table 4.16: Sources and methodologies for network characteristics.

Chapter 5

Simulations

This chapter details the simulations performed with the objective of addressing the research questions. Sensitivity analyses are also conducted on parameters identified as important. The simulations aim to answer the following questions: *"What fuels play a central role in the future energy system, and in what sectors?"* and *"What are the advantages of a hydrogen network in Europe, and how should it be designed?"*. In these scenarios, imports of fossil resources are permitted, while imports of renewable resources like hydrogen or ammonia are not. This approach is motivated by the goal of analyzing Europe's potential to meet its demand with renewable sources in a self-sufficient manner, compared to previous and current fossil-based energy supply approaches.

The reference scenario corresponds to a net-zero emissions case, where the multiplication factor tc_{mul} for hydrogen exchanges is set to 2. Additionally, an extra multiplication of 1.5 is applied to the upper bound on the maximum transfer capacity of the connection between the Iberian Peninsula and France. This additional factor is based on the results from section 6.2.2 and figure C.2. The value of 2 is chosen as a compromise between system cost gain and the time and resources required for constructing the hydrogen infrastructure. The supplementary factor accounts for the observation that the connection between the two regions is frequently overloaded. Negative CO₂ technologies are not included in the model, as coherent CO₂ storage capacities are not yet assessed and integrated into the model. The aim is to identify more complex but useful mechanisms for reducing EU emissions, considering the uncertain characteristics of future CO₂ capture technologies. Besides, this is in continuity with EnergyScope MC's philosophy of not considering CO₂ negative emissions technologies.

5.1 Scenarios

To conduct a comprehensive system analysis, two series of scenarios are considered. The first series involves increasing CO₂ emissions restrictions for each individual country, ranging from 0 to 100% reduction compared to 1990 levels. The second series of scenarios

focuses on increasing the multiplication factor tc_{mul} for hydrogen exchange from 0 (no hydrogen exchange) to 7, with increments of 0.5. The multiplication factor modifies the maximum bounds for hydrogen pipeline capacities connecting regions, with reference values provided in table 4.16. The scenario names are " tc_{mul} x," where x represents the multiplication factor. Notably, the reference transfer capacity for the Iberian Peninsula/France hydrogen exchange is further multiplied by 1.5.

5.2 Sensitivity Analysis

5.2.1 Discount rate

Using discount rates in energy modeling allows for taking the value of cash flows taking place at different times into account. It allows for comparing investment, occurring once in a technology lifetime, and yearly operating cost, but also for comparing technologies with different lifetimes. In our case, the discount rate is used as a cost of finance and is useful to annualize streams of payment having different characteristics in the following manner :

$$Total\ Cost_{/year} = \tau C_{inv} + C_{op}$$

, and

$$\tau = i_{rate} \frac{(1 + i_{rate})^{lifetime}}{(1 + i_{rate})^{lifetime} - 1}$$

, with $Total\ cost_{/year}$ the annualized cost of a technology, $lifetime$ the lifetime of the technology and i_{rate} the discount rate. From the formula, it is possible to understand that a high discount rate will lead to a relatively high value for the annualized cost, especially for technologies with high upfront costs. Renewable technologies, nuclear, and energy efficiency actions are in general capital intensive, though they imply low operation costs, contrarily to fossil technologies. Therefore, high discount rates generally favor fossil technologies over renewable ones.

The value of the discount can be seen as a cost of capital, which depends on factors such as the source of funding, the interest rates of borrowed capital, the expected rate of return in the sector, risks, individual or company investment, etc. According to the report of the EU 2020 reference scenario (using PRIMES model), typical discount rate values are, for example, 7.5% and 9.5% for the industrial/energy sector and public transport sector respectively, while it can go up to 11% for individual home heating equipment. As these values can vary depending on various factors but also due to the fact that only one value can be used for all technologies in EnergyScope, it has been decided to perform a sensitivity analysis. For this analysis, values are taken in the range of 5 to 10 %.

Conceptually, the discount rate is used to model individual decision-making based on the perception of the time-depending value of money and the resulting system is therefore designed as such. This type of discount rate called the private or financial discount rate is differentiated from the social discount rate, which represents the value that the community as a whole gives to the future.

5.2.2 Methanol exchange capacities

It has been observed that the system uses methanol exchange as a substitute for hydrogen, gas, and electricity exchanges in regions with high renewable potential, due to the transfer capacity limitations of these energy vectors. However, methanol is exchanged as freight, with the limitation that the related means of transportation have. It is hardly conceivable to exchange 25 GW of methanol continuously via truck, train, and waterways when it is known that, in the model, only half of that transfer capacity for electricity is allowed between Spain and France, which is already 4 times bigger than the current existing capacity. It has therefore been decided to conduct a sensitivity analysis of the system with a smaller transfer capacity for the energy vectors transported as freight, by setting a maximum transfer capacity of 6 GW.

Chapter 6

Results and discussion

6.1 System Design

This section provides an overview of the system design for the reference scenario and compares it with a scenario with emissions equivalent to those in 1990. Figure 6.1 illustrates the Sankey diagram for the reference scenario, showcasing the layers, technologies used, end-use demands, and the connecting fluxes.

To get rid of CO₂ emissions, a massive electrification of the system is required. Electricity, which is produced in majority by solar and wind technologies, is not only needed for direct use in the mobility and the heating sectors but also as the primary energy source for methanol, ammonia, and synthetic fuels production. Hydrogen is also heavily required as an intermediate energy vector for methanol and ammonia production but is also directly used in road freight transportation. It is also used in steel production and aviation to a lesser extent. Electricity is massively produced from solar and wind technologies, and from nuclear, hydro and geothermal power-plant to a lesser extent. Biomass is largely used for the production of methanol and methane.

Figure C.1 shows that the system with 0 emission reduction imports large amounts of fossil fuels. Coal amounts to a bit less than 50% of the total electricity production. This electricity production falls down to 4550 TWh compared to 10070 TWh in the 100% renewable scenario. In 2021, the quantity of electricity produced in the regions considered was 2750 TWh¹. This low level of production compared to what is designed by the model in both scenarios is due to (I) the high attractiveness of electric heat pumps for domestic heating in EnergyScope, while fossil fuels are practically more used in reality, (II) the intense use of electricity in the road mobility sector and for hydrogen production, (III) the increased energy demand in 2035 compared to 2021.

¹Eurostat data code : NRG_IND_PEH

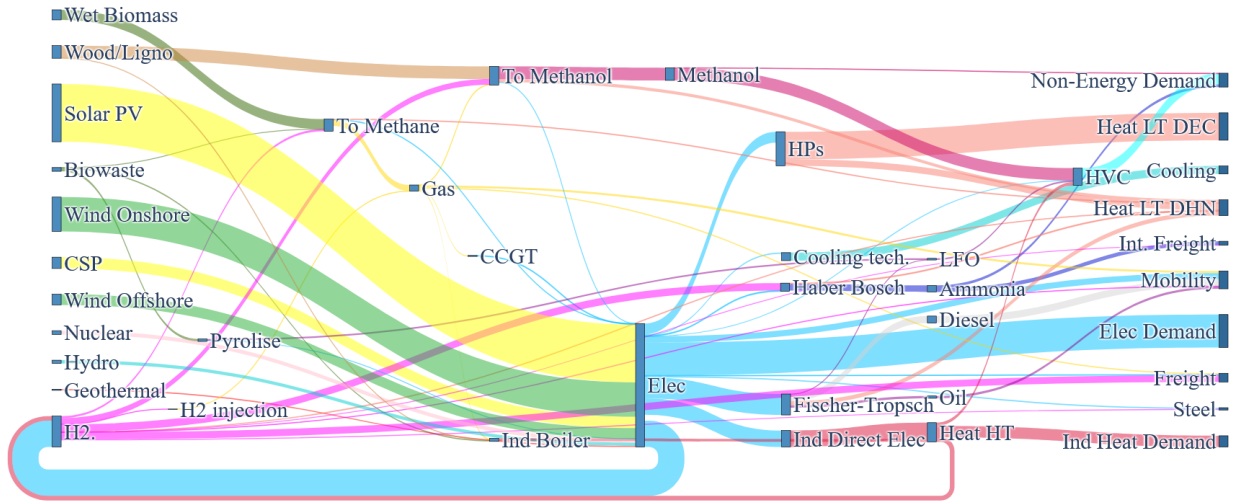


Figure 6.1: Sankey diagram for the yearly operation of the global optimized system, with 0 CO_2 emissions.

6.2 System Cost

The previous section emphasizes the necessity of ambitious electrification targets, which entails investments in renewable electricity production technologies, conversion technologies, and suitable end-use technologies. Additionally, it requires enhanced storage capacities and robust grid infrastructures to accommodate intermittent energy sources. This section aims to highlight the sectors requiring the most significant investments to achieve electrification targets. It also seeks to develop an understanding of CO_2 mitigation options, their effectiveness in reducing emissions, and their cost-effectiveness.

6.2.1 Impact of CO_2 Emissions Reduction

Figure 6.2 illustrates the evolution of system costs in $\text{b}\text{€}/\text{year}$, encompassing discounted investment costs and annual operation and maintenance costs, as CO_2 emissions decrease. This figure serves as a foundation for comprehending various system design possibilities and their implications on emissions and costs.

The cost trajectory can be divided into two segments: from 0 to 50% reduction and from 50 to 100% reduction. The cost increase in the first segment is relatively small, while it is much more substantial in the second segment. In the initial segment, the reduction in CO_2 emissions is achieved by substituting a portion of coal-based electricity production with renewables and gas based electricity. However, this does not constitute true electrification, as total electricity production remains relatively unchanged. The second segment represents the electrification phase, with electricity production increasing by 900 TWh in the first reduction quarter and reaching 10070 TWh in the reference scenario. Biomass is also maximally utilized, except for waste, which is not employed in the strictest scenarios.

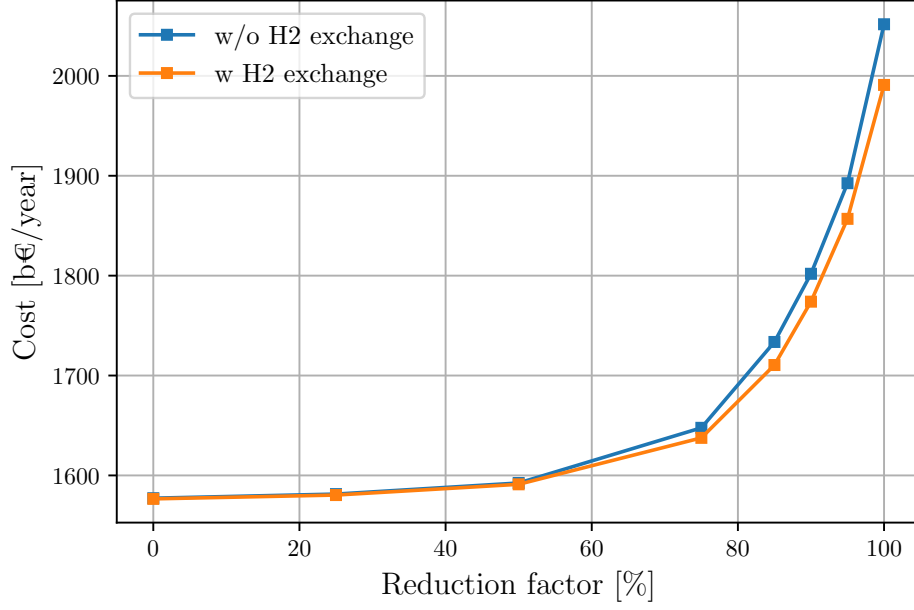


Figure 6.2: Evolution of system total price with increasing percentage of CO_2 emissions reduction, compared to 1990.

Figure 6.3 provides insights into the sectors most impacted by the decarbonization process. Transitioning from 0 to 100% emission reduction results in a system cost increase of 414 b€/year in the reference scenario. The distribution of costs across sectors and infrastructures is illustrated in the figure.

The electrification of the system necessitates an additional cost of 313 b€/year for the expansion of renewable electricity production technologies. These technologies rely on intermittent energy sources, thus requiring grid reinforcement and storage facilities, contributing to an indirect cost of 192 b€/year. Conversion technologies play a role in transforming electricity into energy vectors suitable for challenging-to-electrify sectors, such as aviation, maritime, and non-energy sectors. Electrolyzers, Haber-Bosch, Sabatier, ammonia production plants, and other conversion technologies contribute to a 154 b€/year increase in system costs. Subsequent to electrification, the mobility and heating/cooling sectors transition to more expensive but efficient technologies, including hydrogen fuel cells and electric vehicles. Additionally, reducing fossil fuel imports enables regions to save 304 b€ per year when comparing the two scenarios.

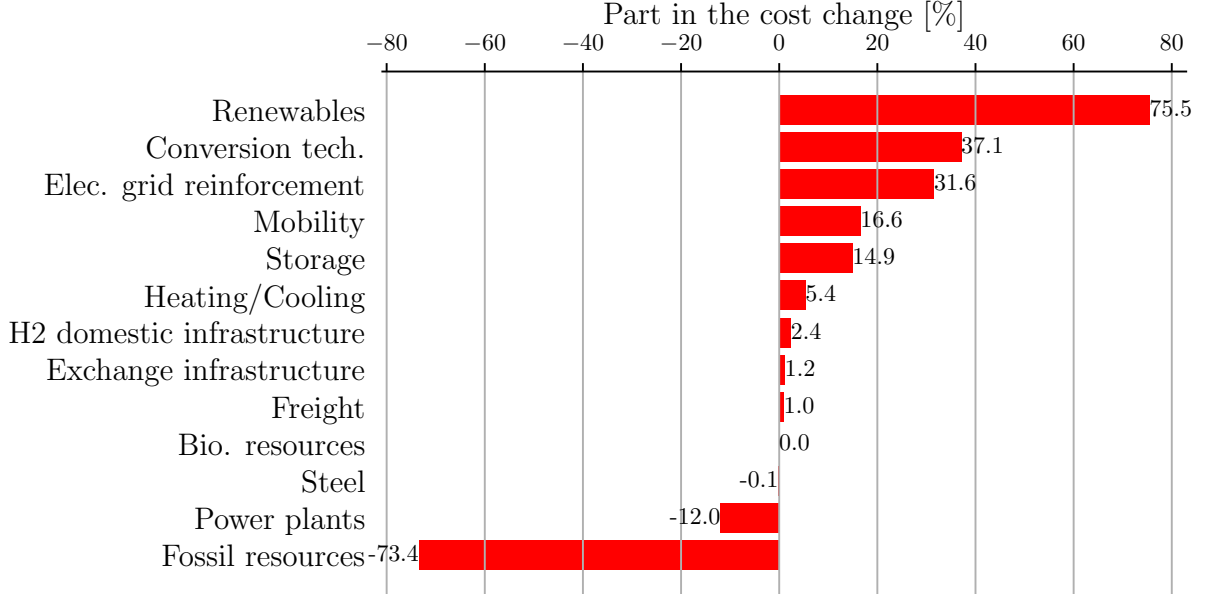


Figure 6.3: Allocation of system cost difference between 0% and 100% CO_2 emissions, categorized by groups.

An alternative approach to understanding the impact of CO_2 emissions reduction is to examine the cost of eliminating the final ton of carbon dioxide from the system to attain the emission target. In the optimization problem, this cost is viewed as the dual value of the CO_2 constraints:

$$\forall c \in \text{REGIONS} \quad (6.1)$$

$$CO_{2, \text{emissions}}^c \leq CO_{2, \text{emissions, max}}^c$$

The dual value of these constraints, one for each region c , represents the change in the objective function (i.e., global system cost) when $CO_{2, \text{emissions, max}}^c$ is incremented by one ton in the considered region. Conversely, the cost of decreasing $CO_{2, \text{emissions, max}}^c$ by one ton—the price of the last ton of CO_2 before reaching the reduction target—is the opposite of this value.

The cost of the final ton of CO_2 to achieve a specified emission target can be linked to the price of CO_2 quotas in the ETS trading system. This cost reflects the expense of decarbonizing the most expensive sectors necessary to meet the target, directly tied to the price of quotas that should be applied to motivate these sectors to invest in decarbonization.

Figure 6.4 depicts the cost of eliminating the last ton of CO_2 in each individual country. Initially, costs across regions are relatively comparable, with the average cost experiencing a notable increase between 85 and 90% reduction. Beyond 90%, France experiences

a sudden escalation in the cost of its CO₂ ton, followed by the United Kingdom, Ireland, Italy and associated countries, BeneLux and Germany. Spain, Portugal, Sweden, and Denmark do not witness such a sharp change in the cost increase rate, attributed to their abundant low-cost renewable potential. Conversely, other regions relying on imports must invest in expensive exchange infrastructures and conversion technologies to decarbonize their last ton of CO₂.

The pronounced cost increase aligns with findings that the last 10% of decarbonization will be the most challenging due to the adoption of emerging, costlier technologies to address the remaining small fraction of demand not yet decarbonized [43]. These technologies, such as ammonia fuel cells for international maritime shipping (Figure 6.8), hydrogen-to-methanol plants (Figure 6.9), and processes for synthetic fuel production (Figure 6.10), emerge between 85 and 100% emissions reduction. In addition to conversion technologies, the demand for storage significantly rises toward the conclusion of decarbonization, further contributing to escalating costs (Figure 6.12). The price of CO₂ for net zero emission scenarios reported by Victoria et al. [44] ranges between 300 and 400 €/ton, lower than the presented values. This discrepancy can be attributed to the absence of Negative Emission Technologies (NETs) in this analysis.

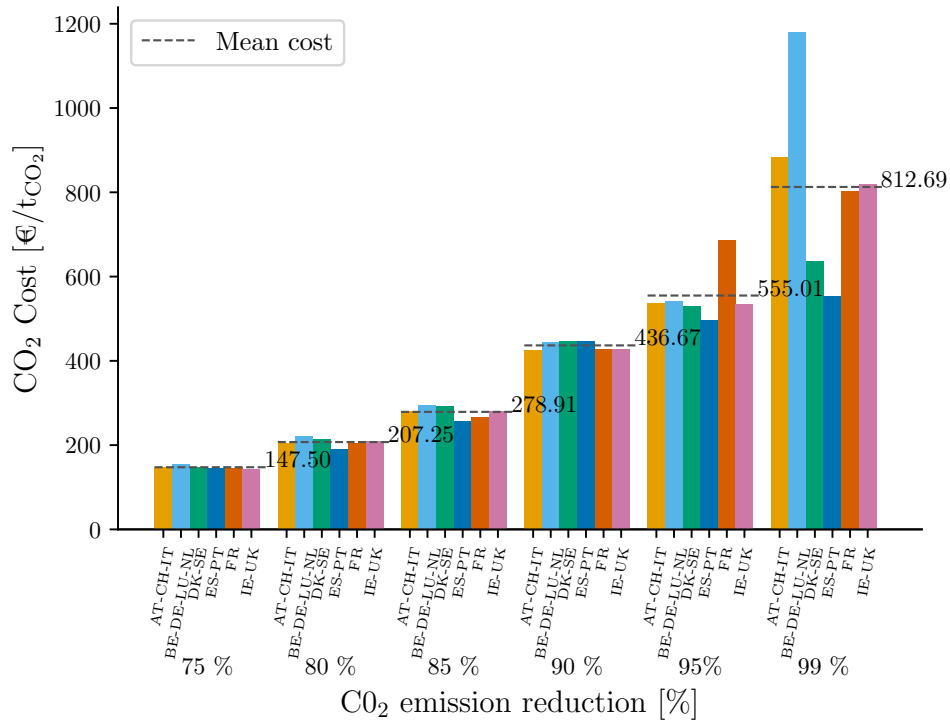


Figure 6.4: Cost of a ton of CO₂ as a function of emissions reduction compared to 1990 levels.

6.2.2 Impact of Hydrogen Network

Figure 6.2 also shows the cost evolution of the system with and without hydrogen exchange capabilities. In the first part of the curve, when no electrification has yet taken place, the hydrogen network is not useful to reduce the cost of the system. It is only beneficial when electrification becomes more important and hydrogen production increases. This is in line with results from Victoria et al. [44] noting that a hydrogen network should appear in 2035, after the decarbonization of the electricity production. In a 100% renewable scenario, it could help decrease the system cost by 60 b€/year, representing 3% of the system without hydrogen exchange. This is in line with findings in [7], where a cost decrease of 3.4% is forecast. However, this number could potentially be higher as EnergyScope does not take into account network bottlenecks in a spatially refined way and geological hydrogen storage, compared to what is done in their analysis. Those are indeed two topics on which a hydrogen network can have a positive impact cost-wise.

As expected, the more the system is allowed to build hydrogen interconnections, the more the system cost decreases, as presented in figure 6.5. As a reminder, the transfer capacities of the interconnections are optimized variables. These variables are constrained between minimum and maximum bounds, the latter being given in tab 4.16. The factor tc_{mul} multiplies the maximum bounds that constrain the transfer capacities of the interconnections. As a results, the bigger the factor tc_{mul} is, the more you allow the system to install a certain amount of interconnection capacity. The question that follows is how much interconnection capacity should be allowed to be built by the system, at maximum. In the figure, the marginal cost decrease related to an increase of 0.5 of the factor tc_{mul} is presented along the cost decrease curve. The marginal cost decrease is expressed in percent of the cost decrease already obtained by the construction of the interconnection capacity allowed by the current value of tc_{mul} . As already stated, it has been chosen to keep a value of $tc_{mul} = 2$ for the reference scenario. Indeed, after this value, the marginal cost decrease falls below 10%, which is quite low and was consider insufficient for the efforts in terms of resources and time necessary to build the connections.

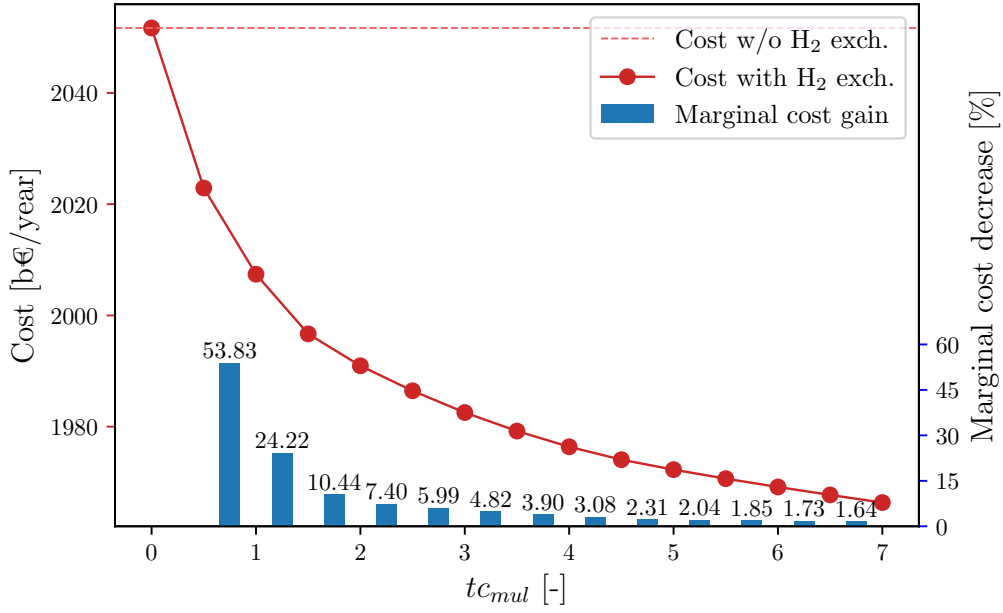


Figure 6.5: Evolution of system price with increasing value for the maximum bound on the transfer capacity for hydrogen. tc_mul is the multiplication factor for the reference capacities of table 4.16. The maximum bound for the transfer capacity between the Iberian peninsula and France is further multiplied by 1.5. The marginal cost decrease is the additional cost gain in percent of the cost gained for the current value of the multiplication factor tc_mul , when considering an increase of this factor of 0.5.

In order to have a better understanding on how the hydrogen network affects the system, one can take a look at figures 6.6 and 6.7. The reduction in the cost is the result of a shift from a renewable gas based system for central Europe to a hydrogen based system. Indeed, without considering hydrogen, gas is the second best energy vector for transporting energy after electricity due to the low transport costs and to its possible consumption in a variety of sectors. Moreover, energy exchanges are of the utmost importance for Belgium, Germany, the Netherlands and Luxembourg which are four of the nine countries in Europe that are very not likely to be able to satisfy their energy demand with their own renewable potential, according to [6]. This situation leads to massive imports of gas from the periphery to the center of Europe.

Without hydrogen exchanges, all the interconnections from Spain to BeNeLux and the Netherlands are saturated. Additionally, the UK, Ireland, Sweden and Denmark already use all their wind potential. To provide energy to the center of Europe, these countries are then forced to install solar technologies, which have low load factors in these regions. This electricity is used to produce gas, which is then exported to central Europe. Note that Italy is also one of the nine countries that is not likely to satisfy its demand on its own, and therefore can not export large quantities of gas. In the exporting countries, gas is produced from biomass but also massively from hydrogen, which necessitates costly industrial plants. Without hydrogen exchanges, gas is therefore brought to the center of

Europe at high cost.

By allowing hydrogen exchanges, larger quantities of energy are able to transfer from south to north with lower production cost. Indeed, solar technologies have higher load factors in the south and no conversion is needed to transform hydrogen into gas. This is why Spain is the only country that increases its renewable installed capacity. Also, hydrogen set the path for more efficient technologies with the use of hydrogen and ammonia fuel cells, but also with the use of hydrogen in the steel making process. The combined effect of energy coming from the south and the reduction in energy needs due to higher efficiency allows countries such as the UK and Sweden to export less energy and therefore reduce their renewable installed capacity.

The cost decrease can be split into the benefiting energy sectors, as done in figure 6.6. Avoiding unnecessary hydrogen to methane conversion plants make up for the biggest part of the cost decrease. The increase of energy efficiency allows for a decrease in electricity needs, leading to lower grid reinforcement costs. The combined effect of energy efficiency and higher load factors in the south leads to lower renewable installed capacities.

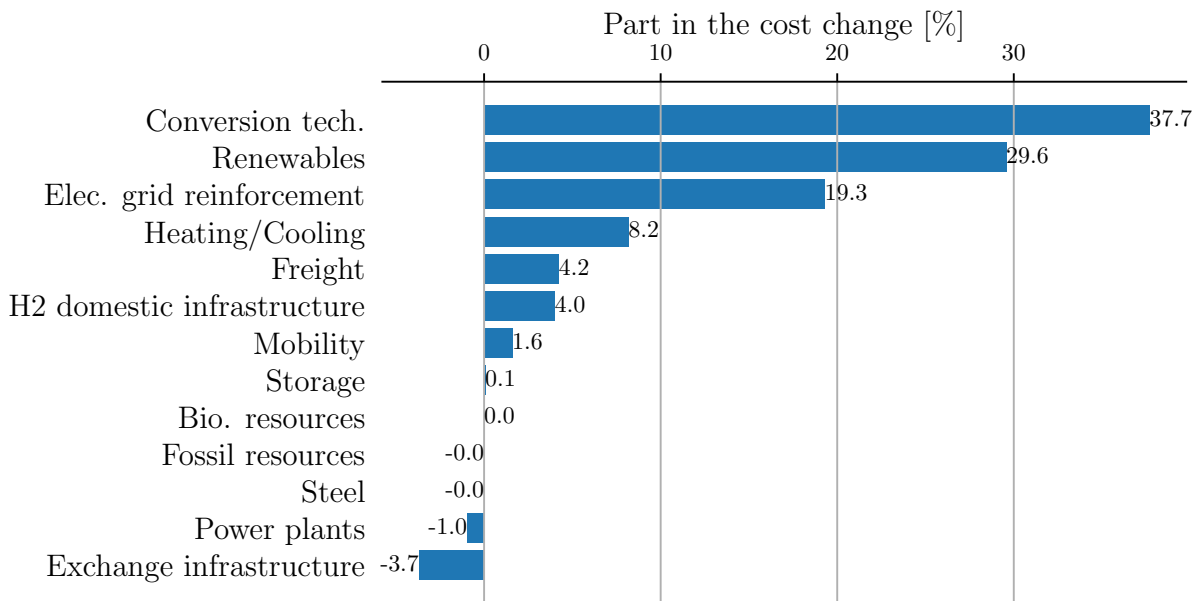


Figure 6.6: Allocation of system cost difference between the with and without hydrogen exchanges scenario, for a net zero scenario, categorized by group.

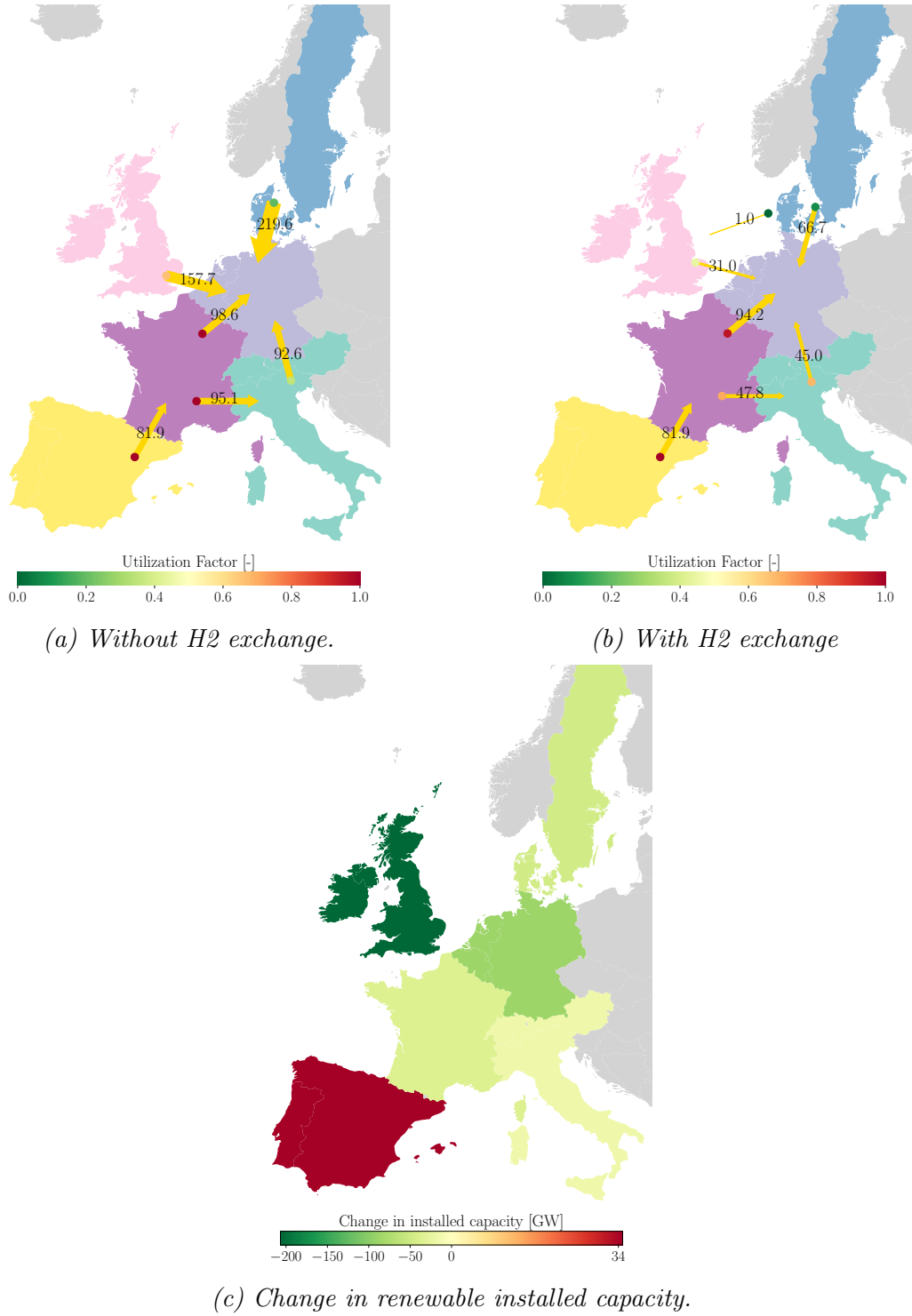


Figure 6.7: Comparison between scenarios with and without hydrogen interconnections, for a 100% emission reduction. Figures 6.7a and 6.7b shows the gas yearly exchange in TWh while figure 6.7c shows the change in the installed capacity of renewable electricity production technologies per country.

6.3 Utilization of renewable fuels

In the previous sections, it has been demonstrated that achieving a net zero-emission Europe relies on the electrification of its energy sectors, either through direct consumption

of electricity or by utilizing electricity-derived energy vectors. While these technologies may entail higher upfront costs, they offer improved energy efficiency and produce minimal direct CO₂ emissions. Additionally, biomass plays a significant role in renewable fuel production.

Different energy vectors can serve the same end-use purposes, but they differ in terms of their source materials, production pathways, storage and transportation feasibility, and the characteristics of the technologies they fuel. As a result, certain renewable fuels are better suited for specific applications. The EnergyScope MC framework enables optimization of end-use technologies, ensuring that the entire chain from production to end-use is optimized. This section aims to elucidate which fuels are most appropriate for given end-uses and the optimal pathways for their production.

6.3.1 Ammonia

Ammonia is exclusively produced from hydrogen, itself derived from electricity. As emissions reduction progresses, ammonia finds application as a fuel for international maritime freight transportation. It offers efficient storage and high propulsion efficiency compared to liquid hydrogen, leading to its expanded utilization. Ammonia production more than doubles, reaching 460 TWh per year. Presently, ammonia is primarily manufactured from natural gas.

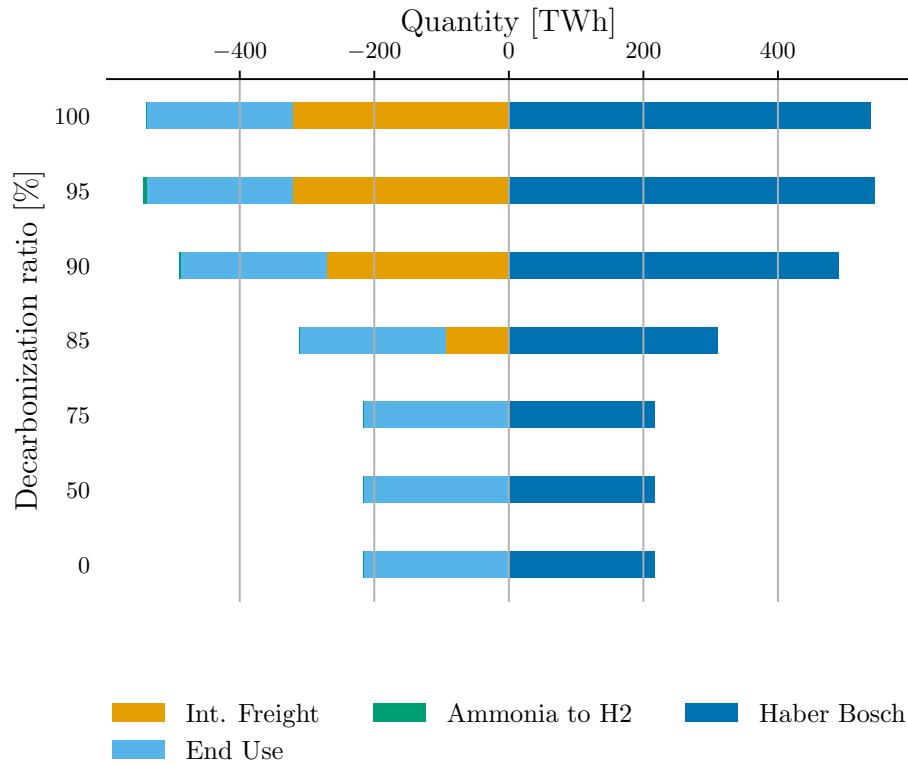


Figure 6.8: Ammonia production methods and consumption sectors.

6.3.2 Methanol

Methanol experiences a substantial surge in consumption during the latter stages of emissions reduction, particularly for the production of high-value chemicals (HVCs). While production from woody biomass remains a preferred pathway, there is a progressive shift away from gas-based production in favor of hydrogen-based production, as imports of fossil gas are reduced. Prior to methanol's ascendancy, HVCs are generated from biomass and imported light fuel oil.

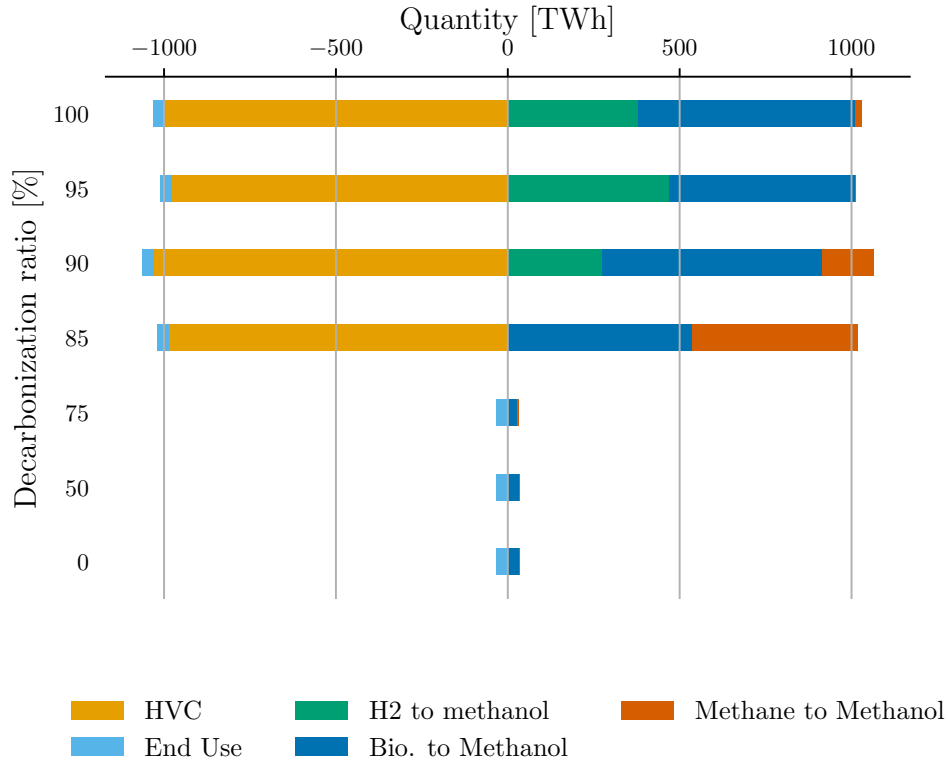


Figure 6.9: Methanol production methods and consumption sectors.

6.3.3 Synthetic Fuel

At the start of decarbonization, pyrolysis is used alongside LFO imports and woody biomass to feed the HVC industry. Indeed, the feedstock for pyrolysis, which is biowaste, is in surplus since coal can be imported at low price to provide industrial heat. At 75% decarbonization, imports of coal are cut out and biowaste is needed for industrial heat, therefore making it unavailable for pyrolysis. As we move on through the decarbonization, industrial heat is electrified and biowaste becomes available again for pyrolysis. Through the decarbonization process, methane is the first synthetic fuel produced after LFO, with its production increasing from 85 to 100% emissions reduction. This is originally produced from wet biomass and is then followed by additional production from hydrogen.

Synthetic diesel and oil/LFO byproducts, produced via the Fischer-Tropsch process,

emerge towards the late stages of decarbonization. The delayed introduction of synthetic fuels underscores the high cost associated with decarbonizing the aviation sector, which is heavily reliant on them.

Synthetic fuels predominantly find application in the mobility sector. While aviation utilizes diesel, natural gas is employed for inland waterway freight transportation and public mobility through natural gas buses. The Fischer-Tropsch process primarily favors the diesel regime in all countries. The gasoline byproduct is employed for private mobility. Pyrolysis-derived LFO is utilized in the non-energy sector.

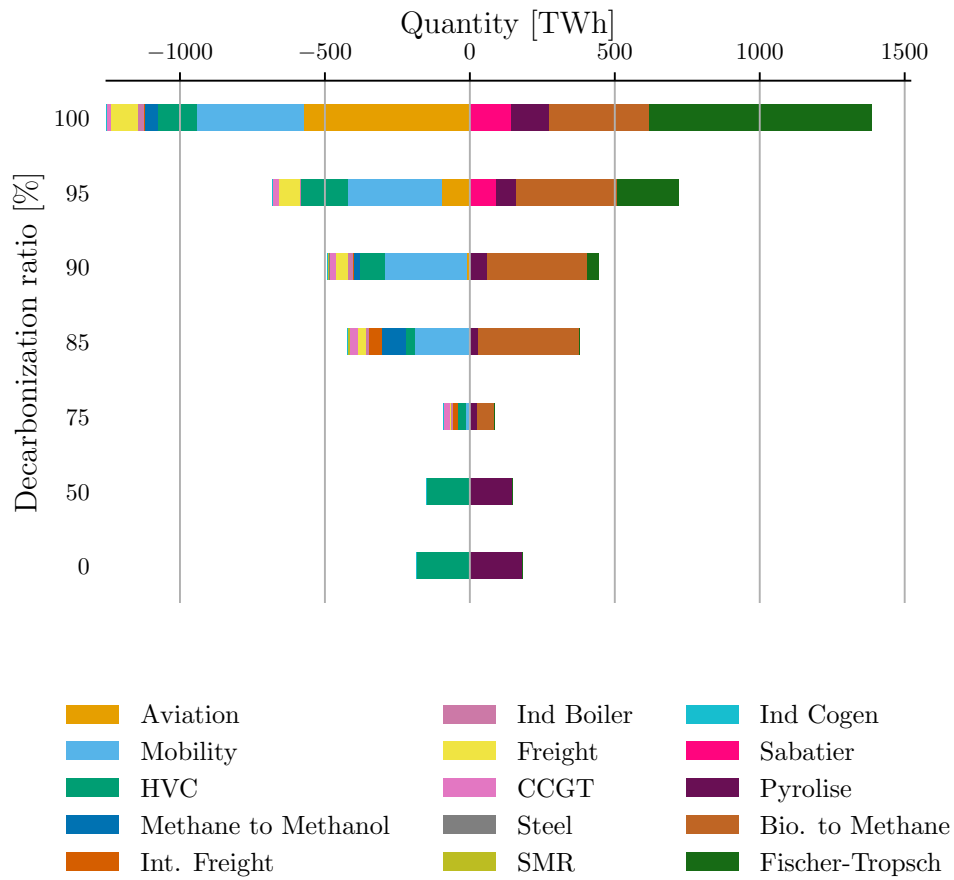


Figure 6.10: Synthetic fuels production methods and consumption sectors.

6.3.4 Hydrogen

Hydrogen is a critical energy vector for facilitating the electrification of the system, experiencing an eightfold increase in production within a fully renewable scenario compared to 1990 emission levels. It is exclusively produced from electricity and serves various roles, including absorbing excess power during peak production periods.

In terms of consumption, hydrogen predominantly serves as an intermediate chemical, facilitating the production of other energy vectors. It is a key input for methanol production within the chemical industry and ammonia production for international maritime

shipping and agriculture. Hydrogen is also directly used in road freight transportation, the steel-making process, and, to a lesser extent, aviation. Towards the latter stages of decarbonization, hydrogen contributes to methane production.

Direct hydrogen utilization amounts to 670 TWh/year, while hydrogen exchanges between countries account for 968 TWh/year. Overall, hydrogen production reaches 1950 TWh annually. Notably, the production of hydrogen required for the Fischer-Tropsch process is not considered in the current analysis or figure, and this aspect should be addressed in future model iterations. However, it has the potential to contribute an additional 1500 TWh, resulting in an overall production of up to 3450 TWh per year within the regions considered. This projection surpasses predictions from most existing models analyzing the net zero scenarios for the EU-28. For instance, projections from the McKinsey Institute, the FitFor55 package, and the JRC TIMES model estimate demand at 1700, 1400, and 1250 TWh/year, respectively [45]. The Hydrogen Backbone consortium and the Pypsa-Eur model estimate higher demands of 2750 TWh/year [36] and around 2500 TWh/year [7], respectively. EnergyScope’s projected demand for the entire EU significantly exceeds these predictions. This difference is attributed to the extensive use of hydrogen-derived fuels in international shipping, agriculture, and the chemical industry, as well as the direct utilization of hydrogen for freight transportation. The optimization algorithm identifies end-use technologies and pathways utilizing hydrogen-derived fuels, offering a clean and efficient approach to fulfilling energy demand while addressing storage and flexibility requirements.

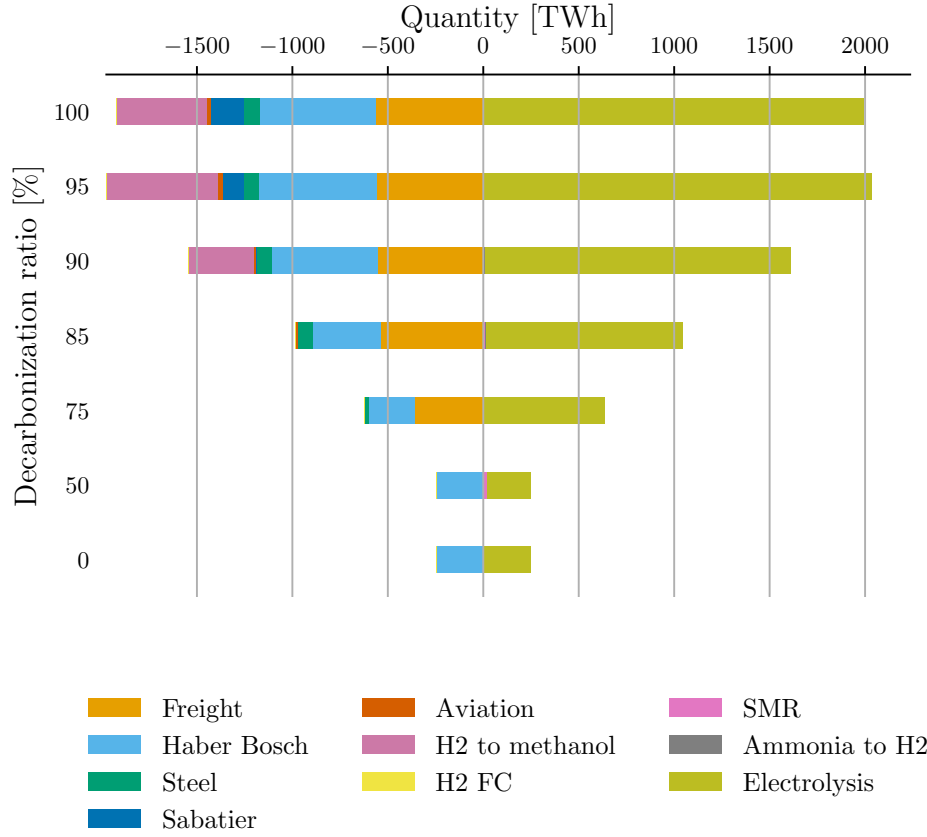


Figure 6.11: Hydrogen production methods and consumption sectors.

6.4 Storage Technologies

Energy storage plays a pivotal role in energy systems by enabling the storage of surplus power during peak production periods and releasing it during periods of high energy demand. This capability enhances the integration of intermittent energy sources into the grid.

Figure 6.12 illustrates the increase in installed capacity of various energy storage technologies throughout the decarbonization process. While certain storage types are better suited for long-term storage purposes, others excel at mitigating intra-day energy production fluctuations. Thermal storage plays a critical role on both seasonal and daily timescales. Notably, the depicted hydrogen storage capacity is lower than the values found in [7]. This discrepancy is attributed to the consideration of only steel tank storage in the present analysis, which is approximately three times costlier than underground storage. Interestingly, the demand for storage, particularly of the chemical type, intensifies after reaching the 80% emissions reduction threshold. This shift is influenced by declining firm electricity production, increased integration of intermittent energy sources, and the expanded production of renewable fuels. A similar trend is observed in [46]. Notably, stationary lithium batteries are not installed in the system, consistent with the scenario

presented in [47], which considered optimal transmission capacities between countries.

It is important to highlight that the conversion of electricity into other energy vectors is unidirectional. Very limited energy is converted back into electricity, as the system does not deploy hydrogen fuel cells. Moreover, Combined Cycle Gas Turbines (CCGTs) are only constructed in central Europe, totaling 78 GW to generate 51 TWh of electricity from renewable gas.

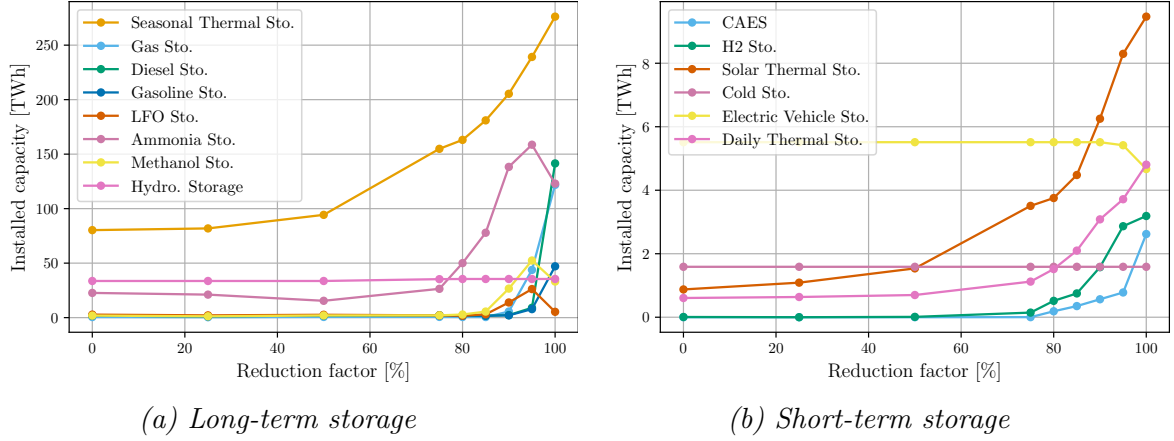


Figure 6.12: System daily and seasonal storage capacities as a function of the decarbonization ratio.

6.5 Energy Exchanges

In addition to storage, energy exchanges are instrumental in addressing the challenge of renewable energy integration. They serve to connect countries with differing production and consumption profiles, ensuring a balanced energy system. Energy exchanges are not only critical for enhancing the self-sufficiency of the EU but also for providing energy at a lower cost to countries with limited renewable potential.

6.5.1 Reference Scenario

Figure 6.13 demonstrates the flow of energy in various forms from the exterior of Europe to its central regions, aligning with the observations made in section 6.2.2. It is important to note that the maximum bound on interconnection capacity is established based on projections from the ENTSO-G TYNDP for gas, electricity, and hydrogen (with a threefold capacity for the hydrogen connection between France and Spain). The optimization model constructs maximum capacity for specific interconnections, highlighting their necessity and underscoring the need for more ambitious interconnection targets.

Moreover, figure 6.13b emphasizes the sustained demand for gas and gas interconnections in the future energy system, even when produced in a CO₂-free manner. Table 6.1

provides insights into the design of newly constructed and repurposed hydrogen interconnections, differentiating between three design types. The first design type involves surplus gas transfer capacity, which can be readily converted to hydrogen capacity. Here, all hydrogen transfer capacity is derived from repurposed gas pipelines. The second design type pertains to critical inter-regional energy transfer routes, exemplified by the Spain/BeNeLux route. For such routes, the optimizer maximizes the available transfer capacity for every energy vector, resulting in the exclusive construction of new hydrogen pipelines, with no repurposed gas pipelines. The third design type represents a compromise between high interconnection capacity and the lower cost of hydrogen pipelines obtained from repurposed gas pipelines. Overall, 45% of the hydrogen exchange network is repurposed from existing gas pipelines, indicating that 21% of the gas exchange network is repurposed. These findings assign a larger share of renewable gas exchanges in the future system compared to other studies. For instance, the EHB proposes that 60% of hydrogen exchange capacity could originate from gas pipelines [40], rising to 69% in [7]. The same study estimates a range of 29% to 49% of the gas network converted into hydrogen pipelines.

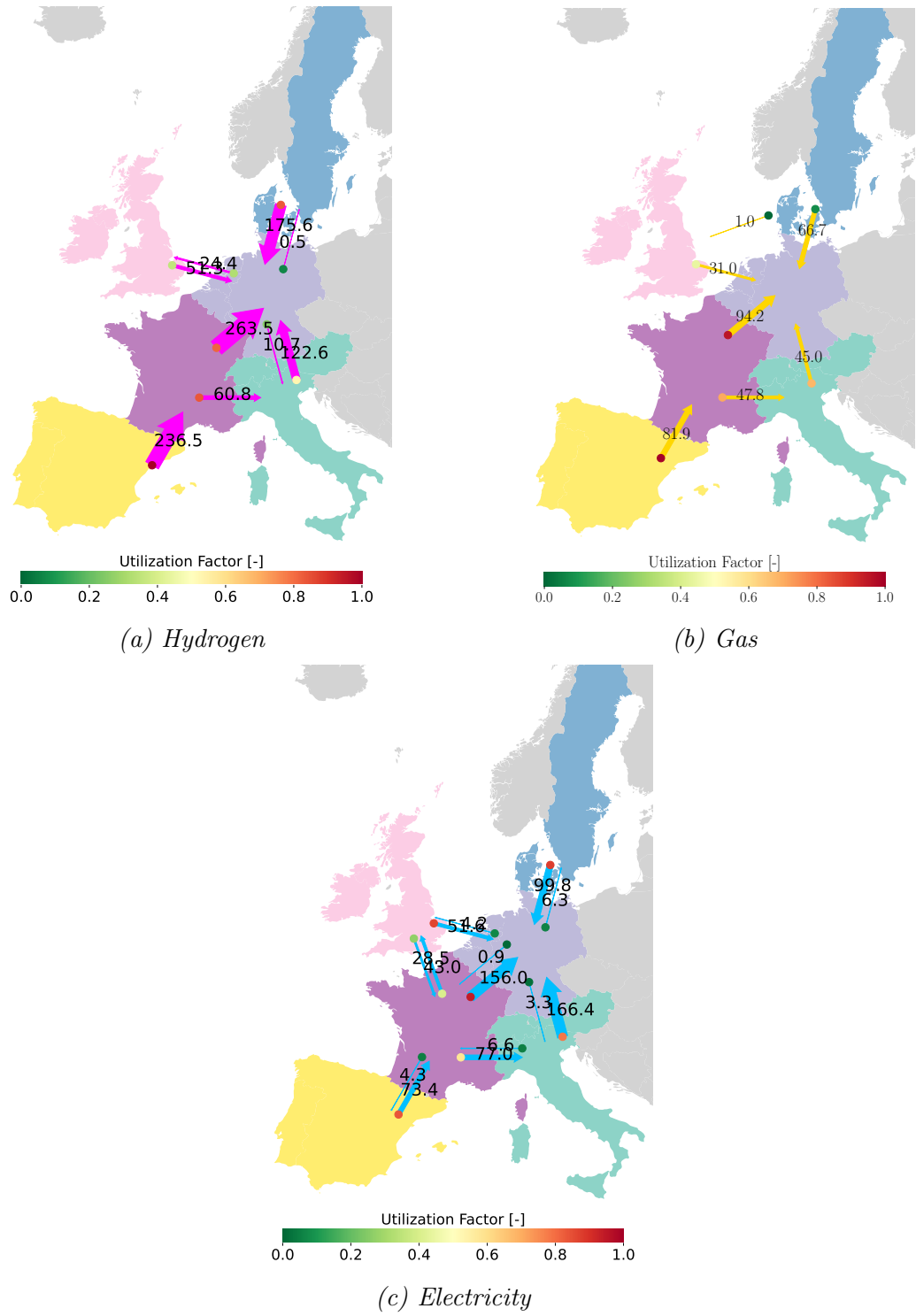


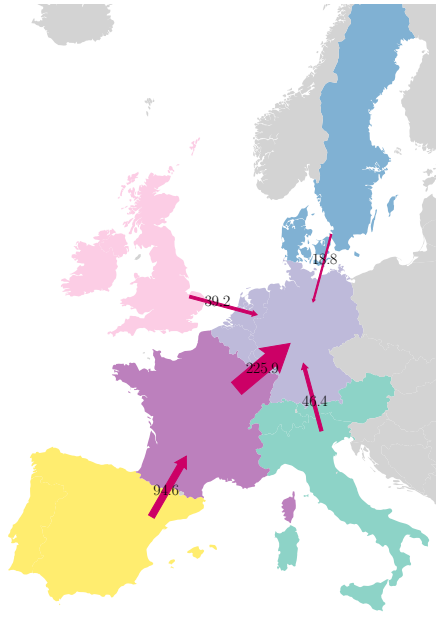
Figure 6.13: Yearly exchange of energy carrier (Hydrogen, gas and electricity) between regions in the reference scenario.

From	To	H ₂ Capa. [GW]	$\frac{H_{2, \text{repurposed}}}{H_{2 \text{ tot}}}$	$\frac{Gas \text{ repurposed}}{Gas \text{ tot}}$
BE-DE-LU-NL	IE-UK	8.65	1	0.23
BE-DE-LU-NL	AT-CH-IT	4.9	1	0.24
DK-SE	BE-DE-LU-NL	24	1	0.26
ES-PT	FR	27	0	0
FR	BE-DE-LU-NL	36.92	0	0
FR	AT-CH-IT	8.33	0.26	0.29
AT-CH-IT	BE-DE-LU-NL	26.5	0.59	0.75
IE-UK	BE-DE-LU-NL	16.67	0.81	0.71

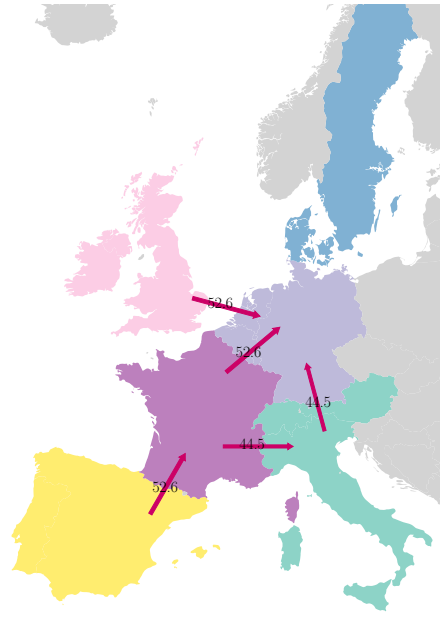
Table 6.1: Gas and hydrogen exchange network design.

6.5.2 Impact of decreasing methanol exchange capacity.

In the reference scenario, large quantities of methanol are exchanged through the northern French border, as shown in figure 6.14. This capacity is equivalent to a constant 25.8 GW interconnection and is assured by freight transportation means. It is seen as quite a logistical challenge as it is equivalent to 2.4 chemical trucks dedicated to methanol transportation traveling from France to BeNeLux every minute. To appreciate the influence of methanol exchange capacity on the system, the maximum capacity of additional freight demand related to energy exchange is set to 6 GW and a comparison to the reference scenario is made in figures 6.14 and 6.15. The result is a significant change in the exchange patterns as methanol exchange is spread out over the Benelux and Germany's neighboring countries. To balance the lack of methanol imports, fewer gas pipelines are converted to hydrogen ones in order to increase energy transfer to central Europe. These changes in the system increase its cost by 0.9%. This highlights the need to develop methanol exchange infrastructures in Europe, especially the one between France and the BeneLux plus Germany region, potentially by considering a methanol pipeline.

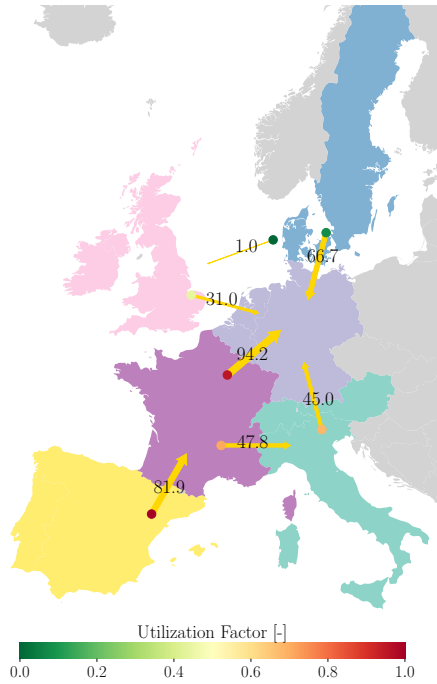


(a) Reference Scenario



(b) $Bound_{max} = 6 \text{ GW}$

Figure 6.14: Yearly exchange of methanol for the reference scenario and when constraining additional freight capacity related to energy exchange to 6 GW.



(a) Reference Scenario



(b) $Bound_{max} = 6 \text{ GW}$

Figure 6.15: Yearly exchange of gas for the reference scenario and when constraining additional freight capacity related to energy exchange to 6 GW.

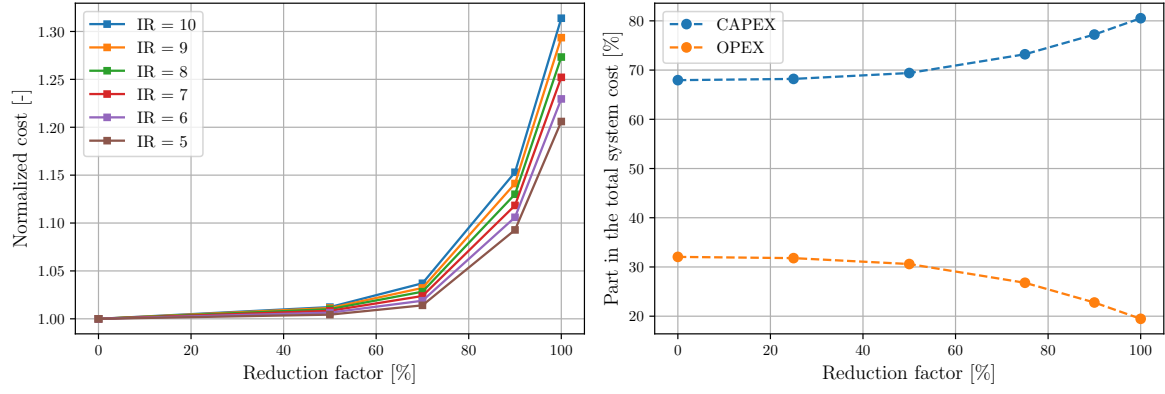
6.6 Impact of the Discount Rate on Decarbonization

Changes in the discount rate have a notable impact on the optimal design and cost of the decarbonized energy system. Figure 6.16 demonstrates that increasing the discount rate

not only leads to higher system costs but also magnifies this effect as higher decarbonization ratios are considered. Notably, when the discount rate is raised to 10%, the cost increase from 0% to 100% emissions reduction is 10% larger than when using a discount rate of 5%. This observation suggests that a higher discount rate acts as a deterrent to decarbonization.

This phenomenon can be understood by examining figure 6.16b. As more stringent emission restrictions are enforced, the optimal system design shifts towards greener electricity production, more intricate pathways for renewable fuel production, and the adoption of emerging and more efficient end-use technologies. Generally, these technologies entail higher investment costs compared to fossil fuel alternatives. Furthermore, the reliance on energy imports diminishes as the system evolves, as these imports typically involve operational expenditures (OPEX) rather than capital expenditures (CAPEX). Consequently, the share of CAPEX in the total system cost increases as the transition progresses towards net zero emissions. Given that the annualization factor amplifies CAPEX when evaluating annualized costs, its impact becomes more pronounced with higher CAPEX values.

In addition to its influence on system costs, the discount rate also shapes the optimal design of the energy system, as indicated in table C.4. Similar trends in system adaptation are observed from 0% to 70% emissions reduction. Notably, the production of hydrogen and the installation of hydrogen-dependent technologies (e.g., fuel cell trucks, Haber-Bosch process plants, ammonia storage) decrease in favor of gas imports and gas-based technologies such as natural gas trucks, gas cogeneration, and Combined Cycle Gas Turbines (CCGTs). The deployment of conversion technologies is also reduced with higher discount rates. The transition from 70% to 90% emissions reduction further accentuates the decline in installed capacity for conversion technologies. During this phase, the system strongly prioritizes direct electrification and the immediate use of hydrogen. Additionally, the focus of gas imports shifts from buses to cargo ships. Finally, at 100% emissions reduction, limited options remain for the system to adapt, as imports are unable to compete with renewable fuels. In this scenario, the system strives to minimize the installed capacity of renewable electricity production technologies while enhancing the deployment of conversion technologies and renewable fuel storage.



(a) Normalized cost.

(b) Part of CAPEX and OPEX in total price.

Figure 6.16: Influence of the discount rate on the system cost (normalized) and the share of CAPEX and OPEX in the total system cost, with increasing decarbonization ratio. For each discount rate, the cost is normalized using the system cost with that discount rate and emissions levels of 1990.

Chapter 7

Conclusion

This study has illustrated that Western Europe has the potential to achieve self-sufficiency in meeting its energy demands with net-zero CO₂ emissions, driven by strong synergies across various energy sectors. This achievement remains attainable even under conservative assumptions regarding energy exchange capacities between countries and without relying on negative emissions technologies. However, reaching such ambitious decarbonization goals comes at a substantial cost, with an increase of 414 billion euros per year compared to the optimal system design with 1990 emission levels. Furthermore, the associated cost of CO₂ abatement for achieving 100% decarbonization reaches 800 euros/ton_{CO₂}, significantly surpassing the current price of approximately 90 euros and the projected price of 300 euros for net-zero emissions in [44].

Renewable fuels play a pivotal role, particularly in the latter stages of decarbonization (above 80%), effectively addressing emissions in challenging sectors. Their utilization results in a substantial increase in system costs due to the adoption of expensive conversion technologies, aligning with the concept of the "last 10%" described in [43]. Biomass and hydrogen contribute significantly to renewable fuel production processes, accounting for 40% and 60% of the processes' inputs, respectively.

The significance of a hydrogen network becomes evident after surpassing the 50% emission reduction threshold, coinciding with the initiation of energy system electrification. In a fully decarbonized scenario, a hydrogen network could lead to a system cost reduction of 3.4% (equivalent to 60 billion euros per year), representing approximately 14.5% of the overall energy transition cost. This reduction is primarily attributed to a decrease in the installed capacity of renewable electricity production technologies across Europe.

Renewable gas and repurposed gas pipelines continue to hold relevance even in a fully decarbonized energy system. Notably, only 21% of gas pipelines are repurposed, contributing to 45% of the future hydrogen exchange network. These findings underscore the importance of renewable gas, deviating from some literature predictions where gas

pipelines constitute 60% to 70% of the hydrogen network through repurposing.

The transformation of electricity into other energy vectors exhibits a one-way process, with minimal reversion back to electricity, barring a few exceptions such as Compressed Air Energy Storage (CAES). Static batteries are not employed for electricity storage. Instead, long-term storage predominantly encompasses thermal and chemical storage solutions. Short-term storage primarily comprises thermal storage and hydrogen storage technologies.

Furthermore, hydrogen’s utilization is predominantly focused on its conversion into other energy vectors, accounting for 80% of its application. Additionally, hydrogen serves direct applications in road freight transportation and steel-making, with a direct consumption of 670 TWh per year. Facilitated by its interregional exchange, hydrogen plays a pivotal role in reducing the overall system cost, with 968 TWh of annual energy exchange. This contribution notably stems from enabling the adoption of energy-efficient technologies in challenging-to-decarbonize regions. Overall, the total annual hydrogen production for Western Europe alone reaches 3300 TWh, surpassing many predictions in the literature.

In summary, this study emphasizes the potential of a synergistic approach to energy system decarbonization in Western Europe. It highlights the critical role of renewable fuels, the significance of hydrogen networks, and the importance of interregional energy exchange. While the cost implications are substantial, the findings underscore the feasibility of achieving ambitious decarbonization goals through holistic energy system integration.

Appendix A

How to extend EnergyScope MC

A.1 How to introduce a new EUD

The first step for adding a new demand is to aggregate the demand data for each region considered. A new line in the file "Demands.csv" located in each region's specific data directory should be created. This line comprises the name of the category and subcategory of the demand, the name of the demand variable in AMPL, the value of the demand for each sector-household, services, industry, and transportation-, and the unit of that value.

The second step is to add the EUTs related to the demand that you want to implement. How to add an EUT is explained in section A.2.

If your demand is time-variable, then its time series should be added in the file "Time_series.csv" of each region's data folder and the column name should be the name of your demand variable in AMPL as set previously in the files "Demands.csv". Afterward, the mapping between the name of your demand variable and the name of its time series variable in AMPL should be done in the file "Misc_indep.json" located in the directory "OO_INDEP". The variable to modify is named "eud_params". Afterwards, you should modify the file "ESMC_model_AMPL.mod" which is the file in which the optimization algorithm is written with the AMPL syntax. Add the parameter for the time series of your demand like this: "param <time_series_name> {REGIONS, HOURS, TYPICAL_DAYS} >= 0, <= 1;".

A.2 How to introduce a new EUT

The link between the EUD and its EUTs is done in the "Misc_indep.json" file located in the "OO_INDEP" directory. The variable concerned is the one related the dictionary key "END_USES_CATEGORIES". Within this variable, add the name of your EUT AMPL variable in the list corresponding to its EUD.

Your EUT will cover part of the demand of its related EUD. The maximum and minimum share of the EUD that your EUT should cover are AMPL parameters that are set in the file "Misc.json" of each region's data directory. After setting the value of these parameters in these files, AMPL parameters with the same names should be created in the file "ESMC_model_AMPL.mod" using these lines : "param share_..._min/max {REGIONS} >= 0, <= 1;". The optimized variable whose value will be constraint between these bounds also needs to be created like this : "var Share_... {c in REGIONS} >= share_..._min[c], <= share_..._max[c];"

Then, since your EUT is a layer, it should appear in every file where layers are relevant. A column with the AMPL name of your EUT should therefore be added in the files "Layers_in_out.csv", "Storage_eff_in.csv", and "Storage_eff_out.csv".

Afterwards, for each EUT, a new "else-if" should be added in the constraint "end_uses_t" in the file "ESMC_model_AMPL.mod", following the syntax of the already considered EUTs.

Finally, the technologies able to provide the demand assigned to your EUT should be added in a way explained in section A.3

A.3 How to introduce a new technology

The first step is to insert the technology characteristics in the file "Technologies.csv" of the region "FR". This region serves as a parent folder for every other regions and you should not add your technology in the file of other regions except if its characteristics are region dependent.

The second and last step is to provide the in- and outflows of your technology in the file "Layers_in_out.csv", i.e the quantities of the layers that are inputs of the technology and the quantities of the layers that are outputs of the technology.

Appendix B

Minor modifications to EnergyScope MC

- Some scenarios would not converge toward a solution. To counter the problem, the following option is added to CPLEX: `densecol=700`. This option sets the minimum nonzeros in a column for the barrier algorithm to consider the column dense. Increasing that value to 700 helped the algorithm to converge.
- Due to the previous implementation of the CO₂ cycle, producing methanol or gas from hydrogen acted as a CO₂ sink. This led to non-logical energy exchange behaviors in which Spain would send hydrogen to France, where it would be converted to gas and sent back to Spain, only to reduce the emissions of France in a cheap manner. The constraint "Minimum_GWP_reduction" and the two technologies in the file "Layers_in_out.csv" have therefore been modified to fix this behavior.
- In the "esmc.py" file, when calling the function "compute_tau", the argument "i_rate" is set to the right value in a dynamic manner and not fixed to a single one. This allows for changing the discount rate without errors in the results.
- The file "Multiplication_factor.csv" had to be created and the relevant changes have been made to the model code to be able to consider different values of the parameter tc_{mul} for each energy vector exchanged via a network.
- The file "Repurposed_cost.csv" had to be created to consider the cost of repurposing gas pipelines for each interconnection and relevant changes have been made to the model code.
- In the "emsc.py" file, additional lines are added to drop some constraints if hydrogen is not allowed to be exchanged between countries.

Appendix C

Additional tables and figures

C.1 Tables

		CAPEX Pipelines [M€/km]	CAPEX Compressors [M€/km]	OPEX Pipelines [M€/year/km]	OPEX Compressor [M€///year/km]
Large	Repurp.	0.5	0.62	0.0045	0.01054
	new	2.8	0.62	0.0252	0.01054
Medium	Repurp.	0.4	0.14	0.0036	0.00238
	new	2.2	0.32	0.0198	0.00544
Small	Repurp.	0.3	0.09	0.0027	0.00153
	new	1.5	0.09	0.0135	0.00153

Table C.1: Summary of pipeline costs, capacities and Capacity- \mathcal{E} distance weighted share of the hydrogen backbone, for different pipeline typologies.

		Proportion in the backbone [-]	Capacity [GW _{LHV}]
Large	Repurp.	0.33	13
	new	0.25	13
Medium	Repurp.	0.19	3.6
	new	0.13	4.7
Small	Repurp.	0.06	1.2
	new	0.03	1.2

Table C.2: Summary of pipeline costs, capacities and Capacity- \mathcal{E} distance weighted share of the hydrogen backbone, for different pipeline typologies.

Country	Rate of increase [%/year]
AT	1
BE	0.7
BG	1.7
CY	2.3
CZ	1
DE	0.8
DK	0.9
EE	1.4
EL	1.3
ES	1.6
FI	1.6
FR	0.7
HR	1.3
HU	1.4
IE	1.2
IT	0.7
LT	1.4
LU	0.7
LV	1.4
MT	2.2
NL	0.6
PL	1.4
PT	0.8
RO	1.7
SE	1.3
SI	1.2
SK	1.2
UK	0.8
CH	0.6

Table C.3: Rate of aviation demand increase.

Technologies	0 % (GW)	50 % (GW)	70 % (GW)	90 % (GW)	100 % (GW)
BIO._TO_HVC	1.37	1.37	-12.96	2.80	0.00
BIO._TO_METHANOL	0.00	0.00	0.00	-4.14	-6.72
BIO_HYDROLYSIS	0.00	0.00	0.00	-46.61	1.06

FT_DIESEL	0.00	0.00	0.00	0.00	24.27
FT_LFO	0.00	0.00	0.00	-3.82	-15.01
H2_ELECTROLYSIS	-55.54	-45.91	-29.51	-8.58	79.54
HABER_BOSCH	-5.38	-6.17	0.00	-19.15	7.84
CH4_TO_METHANOL	0.00	0.00	0.00	-8.75	8.25
METHANOL_TO_HVC	0.00	0.00	0.00	-3.50	0.00
OIL_TO_HVC	-1.37	-1.37	12.96	0.00	0.00
PYRO_BIOWASTE_LFO	-2.94	-20.17	-3.93	0.00	0.00
SMR	29.79	29.88	0.00	-2.97	0.00
SYN_METHANATION	0.00	0.00	0.00	0.00	15.97
SYN_METHANOLATION	0.00	0.00	0.00	8.22	1.66
CARGO_FC_AMMONIA	0.00	0.00	0.00	-543.49	111.66
CARGO_FC_LH2	0.00	0.00	0.00	89.39	-111.65
CARGO_LNG	0.00	0.00	0.00	454.09	0.00
TRUCK_FUEL_CELL	-352.85	-273.22	-729.78	38.00	23.13
TRUCK_NG	352.84	274.12	727.64	0.00	0.00
DEC_BOILER_GAS	347.63	7.76	0.00	0.00	0.00
DEC_DIRECT_ELEC	0.00	0.00	0.00	109.56	0.00
DEC_HP_ELEC	-329.51	-7.55	0.00	-71.10	0.00
DHN_COGEN_GAS	9.91	73.44	0.00	0.00	0.00
DHN_DEEP_GEO	0.00	-9.29	0.00	-21.03	0.00
DHN_HP_ELEC	-23.65	-73.40	-5.22	34.73	-2.42
IND_BOILER_BIOWASTE	3.60	24.72	7.71	-2.63	-4.51
IND_BOILER_COAL	-12.33	-35.47	-49.15	0.00	0.00
IND_BOILER_GAS	0.00	0.00	0.00	-51.87	-27.03
IND_BOILER_WASTE	0.00	0.00	-3.33	49.43	0.00
IND_BOILER_WOOD	0.00	2.83	29.81	0.00	29.94
IND_COGEN_GAS	0.00	0.00	7.17	0.00	0.00
IND_DIRECT_ELEC	0.00	0.00	-9.36	-14.30	25.29
BUS__CNG_STOICH	0.00	0.00	0.00	-570.76	125.98
BUS__FC_HYBRIDH2	0.00	0.00	0.00	0.00	67.56
CAR_BEV	0.00	0.00	0.00	0.00	-9.77
CAR_GASOLINE	0.00	0.00	0.00	0.00	9.77
TRAIN_PUB	0.00	0.00	0.00	615.87	-208.82
DHN	-7.20	-9.23	-5.23	13.70	-2.43
H2_GRID_COMPRESSOR	-25.64	-18.92	-52.15	3.69	38.14
H2_GRID_PIPELINE	-25.64	-18.92	-52.15	3.69	38.14
CCGT	-44.27	80.97	26.48	7.79	0.00
COAL_US	43.21	-79.66	0.00	0.00	0.00
NUCLEAR	0.00	-11.32	0.00	0.00	0.00

PV_ROOFTOP	0.00	0.00	0.00	0.00	-65.14
PV_UTILITY	-487.70	-29.99	-218.41	773.41	-32.10
ST_COLLECTOR	226.53	209.46	411.46	-981.71	219.35
ST_POWER_BLOCK	46.35	26.59	45.07	-124.45	39.78
WIND_OFFSHORE	-15.86	-32.67	26.40	-54.91	0.00
WIND_ONSHORE	-258.26	-474.10	-167.38	187.28	22.76
COAL	766572.03	-1309115.04	-441004.36	3.58	0.00
DIESEL	0.00	2.58	2.45	-8262.44	0.00
GAS	1518070.35	2347645.62	496575.15	-286380.64	0.00
GASOLINE	0.00	1.35	1.48	0.00	0.00
LFO	55.45	128298.20	235734.65	4.12	0.00
METHANOL	0.00	4.23	8.35	0.00	0.00
OTHER_LIGNO	45165.63	28653.02	4616.76	0.00	0.00
URANIUM	-10.72	-227456.80	0.00	0.00	0.00
WASTE	-165.66	8.31	-25239.38	228863.86	0.00
WET_BIOMASS	1.24	22.02	154.73	-767436.65	0.00
WOOD	6305.57	27315.00	0.00	0.00	0.00
AMMONIA_STORAGE	-17215.95	-19815.70	-4212.90	-30594.99	12449.57
CAES	0.00	0.00	0.00	411.54	-311.06
DAM_STORAGE	-1497.52	-1500.25	-1497.40	0.00	0.00
DIESEL_STORAGE	-333.43	572.47	111.63	-281.30	-3568.78
GASOLINE_STORAGE	-332.66	571.17	111.36	-233.89	-699.96
GAS_STORAGE	-136.66	186.21	0.00	-6457.50	-10012.89
H2_STORAGE	0.00	0.00	-72.00	191.56	433.36
LFO_STORAGE	-837.69	-997.09	111.34	-3986.73	-3479.09
METHANOL_STORAGE	-332.65	571.14	111.35	-2456.71	6450.94
PHS	0.00	0.00	-83.59	817.28	-193.25
ST_STORAGE	-333.35	289.84	347.05	-4219.52	874.56
TS_DEC_BOILER_GAS	173.69	0.00	0.00	0.00	0.00
TS_DEC_DIRECT_ELEC	0.00	0.00	0.00	353.63	0.00
TS_DEC_HP_ELEC	-500.47	-30.30	-206.31	38.41	-21.73
TS_DHN_DAILY	0.00	0.00	0.00	0.00	436.51
TS_DHN_SEASONAL	-58556.94	-65340.16	-32149.31	-15105.19	6290.65
TS_HIGH_TEMP	0.00	0.00	0.00	-33.35	25.19

Table C.4: Change in the installed capacity of various technologies and in energy import quantities when changing the discount rate from 5 to 10%, for various emissions reduction targets.

C.2 Figures

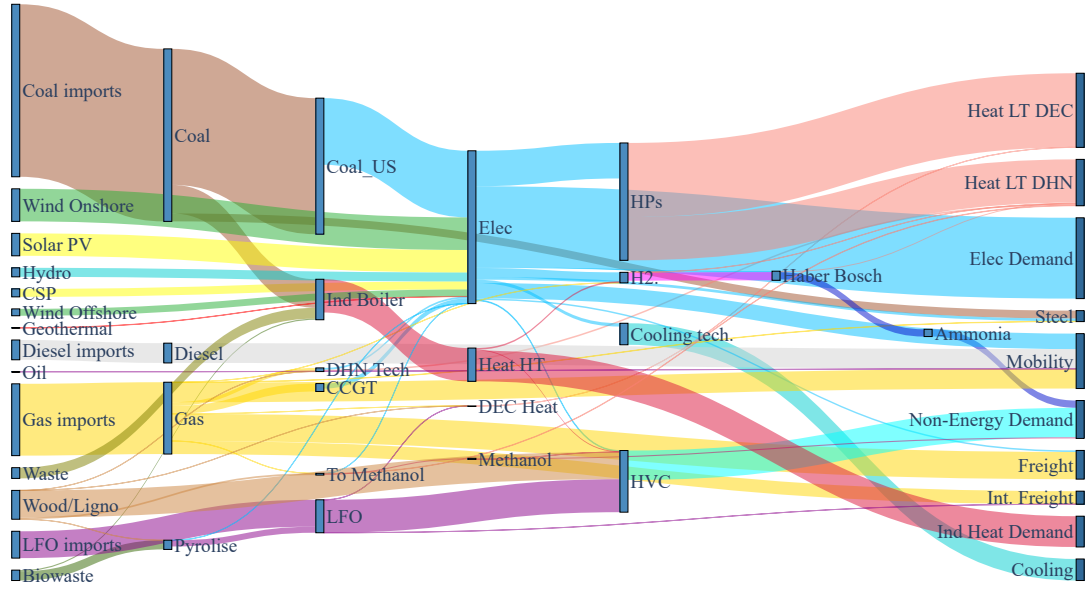


Figure C.1: Sankey diagram for the yearly operation of the global optimized system, with CO_2 emission levels of 1990.

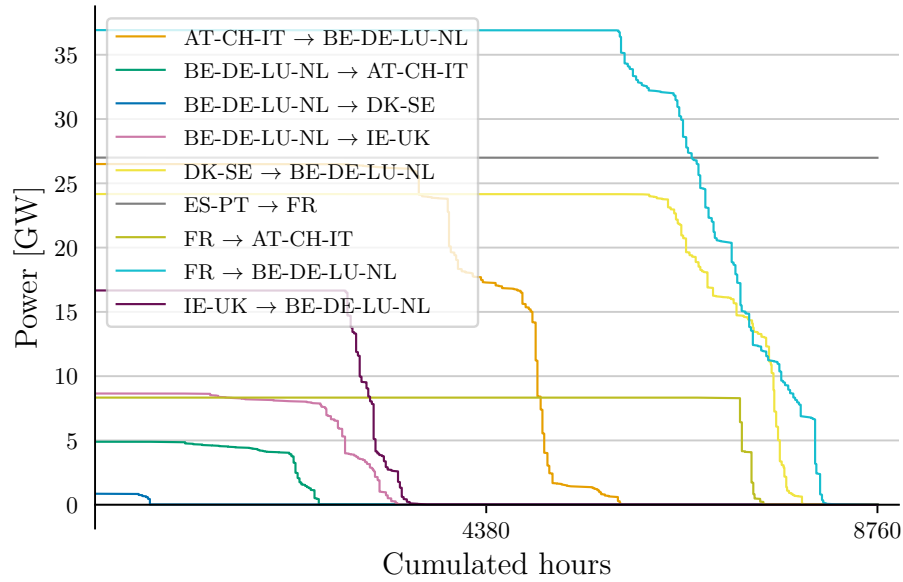


Figure C.2: Cumulated load profile of hydrogen interconnections for a value of tc_{mul} equals to 2.

Bibliography

- [1] *Council decision (EU) 2016/ 1841 - of 5 October 2016 - on the conclusion, on behalf of the European Union, of the Paris Agreement adopted under the United Nations Framework Convention on Climate Change.*
- [2] European Comission. *The European Green Deal.*
- [3] *Regulation (EU) 2021/1119 of the European parliament and of the council of 30 June 2021 establishing the framework for achieving climate neutrality and amending Regulations (EC) No 401/2009 and (EU) 2018/1999 ('European Climate Law').*
- [4] European Comission. *'Fit for 55': delivering the EU's 2030 Climate Target on the way to climate neutrality.*
- [5] European Comissions. *REPowerEU Plan.*
- [6] Jeroen Dommisse and Jean-Louis Tychon. *Modelling of low carbon energy systems for 26 european countries with EnergyScopeTD : can european energy systems reach carbon neutrality independently ?* 2019. URL: <http://hdl.handle.net/2078.1/thesis:25202>.
- [7] Fabian Neumann, Elisabeth Zeyen, Marta Victoria, and Tom Brown. *Potential Role of a Hydrogen Network in Europe.* 2023. DOI: 10.1016/j.joule.2023.06.016.
- [8] Karlo Hainsch, Thorsten Burandt, Konstantin Löffler, Pao-Yu Oei, and Christian von Hirschhausen. *Emission Pathways Towards a Low-Carbon Energy System for Europe - A Model-Based Analysis of Decarbonization Scenarios.* 2018. URL: <https://www.researchgate.net/publication/326370065>.
- [9] Sofia Simoes, Wouter Nijs, Pablo Ruiz, Alessandra Sgobbi, Daniela Radu, Pelin Bolat, Christian Thiel, and Stathis Peteves. *The JRC-EU-TIMES model: Assessing the long-term role of the SET Plan Energy technologies.* 2019. DOI: 10.2790/97596.
- [10] Matteo Giacomo Prina, Benedetto Nastasi, Daniele Groppi, Steffi Misconel, Davide Astiaso Garcia, and Wolfram Sparber. *Comparison methods of energy system frameworks, models and scenario results.* 2022. DOI: 10.1016/j.rser.2022.112719.
- [11] Stefano more, Michel Bierlaire, and François Maréchal. *Strategic energy planning under uncertainty: a Mixed-Integer Linear Programming Modeling Framework for Large-Scale Energy Systems.* 2016. DOI: 10.1016/B978-0-444-63428-3.50321-0.

- [12] Gauthier Limpens, Stefano Moret, Hervé Jeanmart, and Francois Maréchal. *EnergyScope TD: A novel open-source model for regional energy systems*. 2019. DOI: 10.1016/j.apenergy.2019.113729.
- [13] Gauthier Limpens. *Generating energy transition pathways : application to Belgium*. 2021. URL: <http://hdl.handle.net/2078.1/249196>.
- [14] Paolo Thiran and Aurélia Hernandez. *EnergyScope Multi-Cell : a novel open-source model for multi-regional energy systems and application to a 3-cell, low-carbon energy system*. 2020. URL: <http://hdl.handle.net/2078.1/thesis:25229>.
- [15] Noé Cornet and Pauline Eloy. *Energy exchanges between countries for a future low-carbon Western Europe : merging cells in EnergyScope MC to handle wider regions*. 2021. URL: <http://hdl.handle.net/2078.1/thesis:33090>.
- [16] Paolo Thiran. *Validation of Methods to Select a Priori the Number of Typical Days for Energy System Optimisation Models*. 2022.
- [17] *Low-Emission Fuel Supply – Analysis - IEA*. URL: <https://www.iea.org/reports/low-emission-fuel-supply>.
- [18] Claus Rud Hansen. *A technical, environmental, and techno-economic analysis of the impacts of preparation and conversion*. URL: <https://cms.zerocarbonshipping.com/media/uploads/publications/Preparing-Container-Vessels-for-Conversion-to-Green-Fuels.pdf>.
- [19] *Final consumption – Key World Energy Statistics 2021 – Analysis - IEA*. URL: <https://www.iea.org/reports/key-world-energy-statistics-2021/final-consumption>.
- [20] *Émissions de CO2 des avions et des navires : faits et chiffres (infographie) | Actualité | Parlement européen*. URL: <https://www.europarl.europa.eu/news/fr/headlines/society/20191129ST067756/emissions-de-co2-des-avions-et-des-navires-faits-et-chiffres-infographie>.
- [21] *Initial IMO GHG Strategy*. URL: <https://www.imo.org/en/MediaCentre/HotTopics/Pages/Reducing-greenhouse-gas-emissions-from-ships.aspx>.
- [22] *Maritime freight and vessels statistics - Statistics Explained*. URL: https://ec.europa.eu/eurostat/statistics-explained/index.php?title=Maritime_freight_and_vessels_statistics.
- [23] *Beyond 20/20 WDS - Affichage de tableau - Escales et données sur la performance : temps passé dans les ports, âge et taille des navires, annuel*. URL: <https://unctadstat.unctad.org/wds/TableViewer/tableView.aspx?ReportId=170027>.

- [24] Riviera - News Content Hub - Green wave: 61% of newbuilds ordered will burn alternative fuels. URL: https://www.rivieramm.com/news-content-hub/green-wave-61-of-newbuilds-ordered-will-burn-alternative-fuels-71876?utm_source=newsletter&utm_medium=email&utm_campaign=Marine%5C%5C%20Propulsion%5C%5C%20%5C%5C%26%5C%5C%20Auxiliary%5C%5C%20Machinery%5C%5C%20Newsletter.
- [25] Laursen R., Barcarolo D., Patel H., Dowling M., Penfold M., Faber J., Király J., van der Ven R., Pang E., and van Grinsven A. *Potential of Ammonia as Fuel in Shipping*. 2022. URL: www.emsa.europa.eu.
- [26] Claus Rud Hansen. *A technical, environmental, and techno-economic analysis of the impacts of preparation and conversion*. URL: <https://cms.zerocarbonshipping.com/media/uploads/publications/Preparing-Container-Vessels-for-Conversion-to-Green-Fuels.pdf>.
- [27] Jaan Soone. *Sustainable maritime fuels. 'Fit for 55' package: The FuelEU Maritime proposal*.
- [28] Grzegorz Pawelec and CF Berthon. *System-Based Solutions for H2-Fuelled Water Transport in North-West Europe Comparative report on alternative fuels for ship propulsion*. 2020.
- [29] Rui Neiva, Gareth Horton, Aleix Pons, Kadambari Lokesh, Lorenzo Casullo, Alexander Kauffmann, Giannis Giannelos, Marta Ballesteros, Max Kemp, and Nina Kusnierkiewicz. *Investment scenario and roadmap for achieving aviation Green Deal objectives by 2050 Final Study*. 2022.
- [30] Eduardo Cabrera and João M. Melo de Sousa. *Use of Sustainable Fuels in Aviation—A Review*. 2022. DOI: 10.3390/en15072440.
- [31] *Eurocontrol: Aviation Outlook 2050 Main Report*. 2022.
- [32] Somers J. *JRC technical report: Technologies to decarbonise the eu steel industry*. DOI: 10.2760/069150.
- [33] Gunther Glenk and Stefan Reichelstein. *Reversible Power-to-Gas systems for energy conversion and storage*. 2022. DOI: 10.1038/s41467-022-29520-0.
- [34] European Commission. *Regulation of the European parliament and of the council on ensuring a level playing field for sustainable air transport*. URL: https://ec.europa.eu/transport/themes/mobilitystrategy_en.
- [35] Ausilio Bauen, Niccolò Bitossi, Lizzie German, Anisha Harris, and Khangzhen Leow. *Sustainable aviation fuels status, challenges and prospects of drop-in liquid fuels, hydrogen and electrification in aviation*. 2020. DOI: 10.1595/205651320x15816756012040.

- [36] Anthony Wang, Jaro Jens, David Mavins, Marissa Moultaq, Matthias Schimmel, Kees Van Der Leun, Daan Peters, and Maud Buseman. *Analysing future demand, supply, and transport of hydrogen - Executive summary*. 2021. URL: <https://transparency.entsog.eu/>.
- [37] European Commission. *Science for policy briefs: Assessment of Hydrogen Delivery Options*.
- [38] *ENTSOG 2050 roadmap for gas grids*. URL: www.entsog.eu.
- [39] Jaro Jens, Anthony Wang, Kees van der Leun, Daan Peters, and Maud Buseman. *Extending the European Hydrogen Backbone*. 2021. URL: <https://transparency.entsog.eu/>.
- [40] Jaro Jens, Anthony Wang, Kees van der Leun, Daan Peters, and Maud Buseman. *EHB: a European hydrogen infrastructure vision covering 28 countries*. 2022. URL: <https://www.ehb.beu/maps>.
- [41] *EU Reference Scenario 2016 Energy, transport and GHG emissions Trends to 2050*. URL: <http://europa.eu>.
- [42] G. Baracchini, L. Bianco, F. Cirilli, T. Echterhof, T. Griessacher, M. Marcos, D. Mirabile, T. Reichel, T. Rekersdrees, H. Sommerauer, European Commission. Directorate-General for Research, and Innovation. *Biochar for a sustainable EAF steel production: final report*. DOI: 10.2777/708674.
- [43] Trieu Mai, Paul Denholm, Patrick Brown, Wesley Cole, Elaine Hale, Patrick Lamers, Caitlin Murphy, Mark Ruth, Brian Sergi, Daniel Steinberg, and Samuel F. Baldwin. *Getting to 100%: Six strategies for the challenging last 10%*. 2022. DOI: <https://doi.org/10.1016/j.joule.2022.08.004>.
- [44] Tom Brown Marta Victoria Elisabeth Zeyen. *Speed of technological transformations required in Europe to achieve different climate goals*. 2022. DOI: 10.1016/j.joule.2022.04.016.
- [45] Tarvydas D. *The role of hydrogen in energy decarbonization scenarios - Views on 2030 and 2050*. 2022. DOI: 10.2760/899528.
- [46] Marta Victoria, Kun Zhu, Tom Brown, Gorm B. Andresen, and Martin Greiner. *The role of storage technologies throughout the decarbonisation of the sector-coupled European energy system*. 2019. DOI: 10.1016/j.enconman.2019.111977.
- [47] T. Brown, D. Schlachtberger, A. Kies, S. Schramm, and M. Greiner. *Synergies of sector coupling and transmission reinforcement in a cost-optimised, highly renewable European energy system*. 2018. DOI: 10.1016/j.energy.2018.06.222.